



ADVANCING TOWARDS LITTER - FREE  
ATLANTIC COASTAL COMMUNITIES  
BY PREVENTING AND REDUCING  
MACRO AND MICRO LITTER

## D.2.2.6 - Report on the potential of imagery coupled with deep learning solutions to monitor strandings of large microlitter on the coastline

WORK PACKAGE 2, ACTIVITY 2, TASK 4



Co-funded by  
the European Union





<b>Work package</b>	WP2
<b>Activity and task</b>	ACTIVITY 2, TASK 4
<b>Date</b>	26 / 11 / 2025
<b>Version</b>	2
<b>Authors</b>	CEDRE (Maëlle NGUYEN, Killian MARTIN--BOUTMY, Camille LACROIX, Kevin TALLEC) and IFP Energies Nouvelles (Denis GUILLAUME, Sébastien ROHAIS)
<b>Participants</b>	CIIMAR (Marisa ALMEIDA and Sara LOURENÇO)

#### DISCLAIMER

This document covers activities implemented with the financial assistance of the European Union. The views expressed herein should not be taken, in any way, to reflect the official opinion of the European Union, and the European Commission is not responsible for any use that may be made of the information it contains.



## Summary

Strandings of mesoplastic fragments (0.5-2.5 cm) and large microplastics (1-5 mm), including plastic pellets, are regularly observed on beaches of the Atlantic area. The objective of the Activity 2 of Free LitterAT work package 2 is to improve and enhance capability for microlitter detection and monitoring. In this context, the task 4 includes the development and testing of methods based on imagery coupled or not, with artificial intelligence to quantify large microlitter (1-5 mm) strandings on the coastline, in the context of the EU-recommended monitoring methodology.

To feed this task, the work conducted by CEDRE with the support of IFP Energies Nouvelles (IFPEN), was divided into two parts, for which the main results are presented below.

### Traditional imagery

First, traditional imagery methods were tested to automatically quantify in the laboratory large microplastics in samples pre-treated to retain only the particles targeted. Samples used for the methods testing are real samples collected using the EU-recommended methodology (MSFD TG-ML, 2023), on the French Atlantic coastline, though the French national monitoring program for mesoplastics and large microplastics on beaches. Two separate software tools (ImageJ and plugIm!) were tested to automatically count and characterise particles morphology on sample photographs.

The study highlighted the importance of the quality of the photos acquisition to obtain relevant results. However, even with high quality photos, the imagery analysis performance was affected by the diversity of particles colours typically found in real samples, which decreased the ability to detect all the particles simultaneously with the tested methods and as a consequence, the results accuracy. This less affected pellets and biobeads that have generally a homogeneous colour.

For the semi-automated ImageJ method, results indicated that the method could potentially be used to optimise the EU-recommended methodology that only targets plastic pellets. This should be confirmed by additional testing on more samples (including samples with biobeads to ensure the ability to distinguish them from plastic pellets), in particular to assess the effect of pellet colours and aging on the capacity to robustly detect all the pellets. On the other hand, the method appears to have no added-value compared to the visual counting of the French monitoring program (which considers all large microplastic types) due to the time needed for processing, control, and validation of the results.

Regarding the automated PlugIm! method, results indicated it could meet the requirement of the EU-recommended protocol, only if samples are pre-sorted to just



retain pellets as the method is able to count a total number of particles but it cannot distinguish the different particle subcategories. So, this method only partially meets the requirement of the French monitoring program (that considers all large microplastic categories). However, the possibility of batch analysis appears to be of great interest as it could allow to gain time for the operator and further work should be conducted to fine-tune the settings for this method to improve the particles detection.

The tested methods present a potential in other contexts. For example, if an analysis of the particles size distribution is needed, both methods can provide precise morphological information on the detected particles. In addition, in the context of analysis of homogenous samples (*e.g* same shape and same colour) as it could be the case after an accidental release of plastic pellets at sea leading to important strandings on the coastline, the methods could allow a rapid counting of the number of particles if the method settings are selected appropriately (in particular with the batch analysis of the PlugIm! method).

### AI-based imagery

Secondly, an Artificial Intelligence (AI)-based solution was tested to monitor large microplastics directly in the field on one of the Atlantic beaches included in the French national monitoring program (Le Stang, Brittany, France). The workflow begins with the acquisition of standardised photos, focusing on wrack-lines where meso- and microplastic concentrations are typically highest due to coastal processes. These photos were used to build a comprehensive learning database. Deep learning model was then trained using this database, followed by a performance evaluation. The workflow extended beyond simple identification and quantification of plastics, incorporating a step to convert the observed abundances into mass estimates. This was achieved using pre-established correlation laws that link morphological parameters to mass.

The main results of this real-case test demonstrated a strong correlation between the results obtained through the photo-based AI analysis approach and those from the standardised French monitoring protocol. Even though the values calculated by the AI, both in terms of mass and number, did not perfectly match those obtained through physical surveys on monitoring networks, they remained highly consistent. The relative proportions between different plastic categories were well maintained—if a particular type of microplastic was more prevalent in physical surveys, the AI analysis of photo data reflects the same trend. Additionally, the temporal variations identified by the AI aligned well with those observed in physical surveys, meaning the AI effectively tracks increases and decreases in meso- and microplastic pollution over time.

Optimizing the acquisition protocol by reducing the number of photos without compromising result quality was also a significant finding of the present work. This can lead to time and resource savings, making large-scale monitoring more feasible in time and space.



Obtained results indicate that the tested method has the potential to meet the requirements of both the EU-recommended and French monitoring program methodologies, in terms of particle counting and characterization and it should be further tested on other monitoring sites with different beach characteristics. However, the photo acquisition strategy on the beach currently differs from the EU-recommended one and it should be further optimised to make the two monitoring approaches more comparable.

Based on its performance in the field, the tested methods also offer interesting perspectives to optimize analyses conducted in the lab, as a complement to the traditional imagery tools such as the ones tested and described above.

Overall, while further studies and improvements are needed, the tested methods have a good potential to optimize the monitoring of large microplastics (1-5 mm) in the context of a routine beach monitoring using the EU-recommended methodology, such as the one conducted on the French coastline, in the context of the the French national monitoring program for mesoplastics and large microplastics on beaches.







# Table of contents

<b>Abbreviations</b>	<b>8</b>
<b>Context: the Free LitterAT project</b>	<b>9</b>
<b>Introduction</b>	<b>10</b>
<b>Part 1: Testing imagery on pre-treated simples</b>	<b>13</b>
<b>1 PRESENTATION</b>	<b>13</b>
<b>2 MATERIAL AND METHODS</b>	<b>13</b>
2.1 Artificial samples	13
2.2 Real samples	14
2.3 Pre-treatment and visual analysis of the samples	15
2.4 Test of image analysis techniques	16
2.4.1 <i>Photo acquisition</i>	16
2.4.2 <i>Test of ImageJ</i>	17
2.4.3 <i>Test of PlugIm!</i>	19
<b>3 RESULTS</b>	<b>21</b>
3.1 Test of ImageJ	21
3.1.1 <i>Analysis of artificial samples</i>	21
3.1.2 <i>Analysis of real pre-treated samples</i>	23
3.2 PlugIm!	26
3.2.1 <i>Analysis of artificial samples</i>	26
3.2.2 <i>Analysis of real samples</i>	28
<b>4 DISCUSSION</b>	<b>31</b>
<b>5 CONCLUSION</b>	<b>32</b>
<b>Part 2: Testing imagery coupled with a deep learning solution directly in the field</b>	<b>34</b>
<b>1 PRESENTATION</b>	<b>34</b>
<b>2 DATA AND METHOD</b>	<b>35</b>
2.1 Photo acquisition – dataset	35
2.2 Integrated workflow	36
2.2.1 <i>Building the dataset for AI</i>	37
2.2.2 <i>Training strategy</i>	38
2.2.3 <i>AI and inference</i>	39
2.2.4 <i>Evaluation Metrics</i>	40
2.2.5 <i>Post-processing cut-off</i>	41
2.2.6 <i>Abundance to mass conversion</i>	41
2.2.7 <i>Comparison with official monitoring results</i>	42



<b>3</b>	<b>RESULTS .....</b>	<b>43</b>
3.1	Abundance of large microplastics and mesoplastics from photo .....	43
3.1.1	<i>Results for 20x20cm quadrats .....</i>	43
3.1.2	<i>Results for 40x40cm quadrats .....</i>	44
3.2	Deep learning solution evaluation .....	45
3.2.1	<i>Training steps .....</i>	45
3.2.2	<i>Validation steps .....</i>	47
3.2.3	<i>Test .....</i>	48
<b>4</b>	<b>DISCUSSION .....</b>	<b>49</b>
4.1	Human factor .....	49
4.2	Database representativeness .....	50
4.3	AI performance and applicability .....	51
4.3.1	<i>Abundance .....</i>	51
4.3.2	<i>Mass .....</i>	53
4.4	Comparison with official monitoring results .....	55
<b>5</b>	<b>CONCLUSION .....</b>	<b>56</b>
<b>References</b>		<b>60</b>





## Abbreviations

A: Area  
AR: 2D Autoregressive  
BLEG: Beach Litter Expert Group  
CNN: convolutional neural network  
EPS: Expanded PolyStyrene  
EU: European Union  
FBF: Fractional Brownian Field  
FTIR: Fourier transform infrared spectroscopy  
GPS: Global Positioning System  
IFPEN: IFP Energies Nouvelles  
MR: Mean Radius  
MSFD: Marine Strategy Framework Directive  
MSFD TG-ML: MSFD Technical Group on Marine Litter  
QC: Quality Control  
RGB: Red, Green, and Blue  
RNS-mP-P: national monitoring network for mesoplastics and large microplastics (1-5 mm) on beaches (Réseau National de Surveillance des mésoplastiques et grands microplastiques (1-5 mm) sur les plages)  
SEM: Scanning Electron Microscopy  
WP: Work Package  
2D: Two Dimension







## Context: the Free LitterAT project

The Free LitterAT project, whose full title is “Advancing towards litter-free Atlantic coastal communities by preventing and reducing macro and microlitter”, is funded by the European Interreg Atlantic program 2021-2027. Lasting 3 years, the project aims to protect biodiversity by implementing innovative approaches to prevent and reduce marine litter pollution. This project, led by CETMAR (Spain), involves 14 partners and 9 associated partners from 4 countries: Ireland, France, Spain and Portugal.

More specifically, the project aims to advance towards litter-free coastal communities by developing, testing and implementing innovative approaches for the prevention, localisation and reduction of marine litter, with a special emphasis on abandoned, lost or discarded fishing gear (also known as ALDFG) and microplastics. The main objectives of the project are:

1. Preventing marine litter by improving waste management and recycling and facilitating the implementation of SUP and PRF Directives;
2. Understanding the origin and location of litter accumulation by identifying major sources, pathways and hotspots of marine litter;
3. Reducing and removing marine litter and associated risks;
4. Promoting litter-free local communities by developing pilot actions and awareness raising activities.

The work is divided into 4 work packages (WP):

**WP 1. Prevention by improving waste management and recycling:** Prevent marine litter by improving waste collection, recycling and increasing awareness in Atlantic ports and coastal cities, with a specific focus on fisheries related waste, for the preservation of the oceans and marine biodiversity.

**WP 2. Assessing and Monitoring micro and macrolitter contamination:** Develop and optimise current tools and methods for monitoring macro and microlitter and to enhance processing and analysis solutions that can facilitate and generate harmonised data that can be integrated into actionable outputs.

**WP 3. Modelling approaches from micro and macrolitter: from modelling outputs to sources and hotspots:** Improve our understanding of the location of accumulation areas of ALDFG, macro and microplastics and their sources, supporting the environmental agencies in charge of marine litter management with powerful modelling tools.

**WP 4. Reducing marine litter and associated risks:** Contribute to reducing marine litter by developing and demonstrating procedures, systems and manuals to remove different types of marine litter (ALDFG, hotspots, microplastics) in different environments.



## Introduction

In the Atlantic area, strandings of mesoplastic fragments (0.5-2.5 cm) and large microplastics (1-5 mm) including plastic pellets, are regularly observed on the coastline (CEDRE, 2024; Rodrigues et al, 2024; Figure 1). Mesoplastic and large microplastic fragments are secondary products which originate from fragmentation of larger plastic objects during their use, recycling or their journey as litter (*e.g.* abrasion, shocks, photodegradation). Plastic pellets (also called plastic nurdles) are the raw material used by the industry to produce a large majority of plastic products. Most plastic pellets are between 2 mm and 5 mm, and are generally white and translucent, even if they can come in a range of colours (CEDRE, 2025).



**Figure 1 : Strandings of mesoplastic fragments (0.5-2.5 cm) and large microplastics (1-5 mm), including plastic pellets, observed on Atlantic French beaches (©CEDRE)**

The size classes and morphological properties of mesoplastic fragments and large microplastic are advantageous in the context of monitoring, as it is relatively easy to collect samples and analyse them in order to identify plastic particles, in particular pellets, and provide an assessment of this pollution. In addition, mesoplastic and large microplastic fragments are considered by some experts to be a better indicator of coastal pollution levels as they are usually not collected during municipalities and citizen clean-ups. Mesoplastic fragments and large microplastics can also be ingested by fauna (*e.g.* seabirds) and their ingestion is currently monitored by international monitoring programs (*e.g.* in the framework of the OSPAR Convention, through the Fulmar ingestion indicator; OSPAR, 2015).

In France, CEDRE has been commissioned by the French Water and Biodiversity Directorate under the French Ministry for Environment, to deploy the national monitoring network for mesoplastics and large microplastics (1-5 mm) on beaches (RNS-mP-P). The first efforts to monitor mesoplastics and large microplastics washed ashore were organised in 2020, when a sampling protocol was tested during opportunistic samplings carried out by CEDRE on the French coastline. Since then, the protocol has been developed and is now implemented in routine through the RNS-mP-P, as part of



the official national monitoring with the objective of collecting data to assess the abundance, composition and trends of pollution by mesoplastics and large microplastics found on the beaches of mainland France, to feed the European Marine Strategy Framework Directive (MSFD).

The methodological development and the experience gained in France on routine monitoring of mesoplastics and large microplastics on beaches, has contributed to the establishment of a harmonised European methodology for monitoring mesolitter fragments and plastic pellets along the European coastline, led by CEDRE in collaboration with Dutch and German experts, in the framework of the MSFD Technical Group on Marine Litter (MSFD TG-ML). This harmonised methodology has been published at the European Union (EU) level in 2023, as part of the updated Guidance on the Monitoring of Marine Litter in European Seas, aiming at improving the harmonised monitoring of marine litter under MSFD (MSFD TG-ML 2023). In parallel, discussions have been launched in the framework of the OSPAR Convention, in the context of the Beach Litter Expert Group (BLEG) led by CEDRE, on the deployment of a similar monitoring initiative on beaches of the OSPAR maritime area.

The methodology recommended at EU level, involves a sampling on survey beaches, four times a year, followed by a manual treatment of the samples in the laboratory to remove the organic matter and sort the pellets and mesoplastic fragments which are subsequently, counted and weighed. This method, still in development, is considered to have a low/medium cost and requiring a medium effort (TG-ML, 2023). This methodology is also the one used in France, except that in the French monitoring, all large microplastics are considered, not only the pellets. To optimise the methodology and reduce its cost and effort, the use of imagery either directly in the field or in the lab, coupled or not with deep learning solutions could be an option.

The objective of the Activity 2 of Free LitterAT work package 2 is to improve and enhance capability for microlitter detection and monitoring. In this context, Task 4 includes the development and testing of methods based on imagery coupled or not, with artificial intelligence (AI) to quantify larger microlitter (1-5 mm) strandings on the coastline.

To feed this task, the work conducted by CEDRE with the support of IFP Energies Nouvelles (IFPEN), is divided into two parts. First, traditional imagery methods were tested to automatically quantify large microplastics in samples pre-treated in the laboratory to retain only the particles targeted. Samples used for the methods testing were real field samples collected using the EU methodology, on the French Atlantic coastline, through the RNS-mP-P. Two separate software tools were tested to assess the potential of traditional image processing techniques to automatically count and characterise particles morphology on sample photographs.

Secondly, a deep learning-based solution was tested to monitor large microplastics directly in the field on one of the Atlantic beaches monitoring under the RNS-mP-P (Le Stang, Brittany, France). To date, there are opportunities to improve the detection and



quantification of microplastics through Artificial Intelligence (AI), particularly in environmental and industrial settings. A pending patent (Rohais et al., 2022) was recently proposed by IFPEN to address these challenges. The resulting workflow has been tested in this study.

For both approaches, results obtained were compared with original monitoring data obtained using the European methodology, in the context of the French national monitoring program for mesoplastics and large microplastics on beaches. On this basis, the performance, the pro&cons and the potential of the tested methods are discussed, taking into account the EU recommendations for monitoring mesolitter fragments and plastic pellets along the European coastline (MSFD TG-ML, 2023).

The present deliverable of the Free LitterAT project (referred as deliverable D.2.2.6) presents the final results of the study. This report is divided into two main parts. The first part describes the development and testing of traditional imagery methods to analyse pre-treated samples in the lab, while the second part focuses on the presentation and testing of the AI-based method developed by IFPEN directly in the field.







# PART 1: Testing imagery on pre-treated samples

## 1 Presentation

To test the potential of traditional image processing techniques to optimise the visual analysis by an operator of samples collected on beaches using the EU methodology for monitoring mesolitter fragments and plastic pellets, two separate tools were selected: ImageJ (Schneider et al., 2012) and, PlugIm! (Tan et al., 2018), freely available online.

The samples considered in the study include 2 artificial samples, prepared by CEDRE but also 5 real samples originally collected in 2024/2025 on the French Atlantic coastline, though the RNS-mP-P, in the context of the French national monitoring program for mesoplastics and large microplastics on beaches. These samples have already been analysed by visual counting, in the context of the official monitoring and were stored at CEDRE. Prior visual counting, the RNS-mP-P samples have been treated to remove the organic matter and retain only the particles targeted, *i.e.* the mesoplastic fragments and the large microplastics (not only the pellets as the French monitoring programme includes all large microplastics such as films, fibers, biobeads and foams). As the mesoplastic and large microplastic fractions were stored separately, it has been decided as a first step, to focus only on the large microplastic fraction of the samples. Mesoplastic fragments are therefore excluded of the present study.

In the present study, photographs of the pre-treated samples were analysed using the two selected softwares and results were compared with the official results obtained by visual counting, in order to assess the relative performance of the imagery methods.

The imagery methods are based on the automatic or semi-automatic detection and analysis of particles number and circularity. The assessment of the relative performance of the methods was done considering the following criteria:

- the capacity of the methods to count accurately the number of plastic particles;
- the ability of the methods to differentiate the plastic pellets from other large microplastics;
- the analysis duration.

## 2 Material and Methods

### 2.1 Artificial samples





Two artificial samples were prepared by CEDRE and used to do the first testing of the imagery methods:

- One sample containing only 50 white plastic polyethylene pellets (obtained from a plastic producer),
- One sample containing 50 white plastic polyethylene pellets (obtained from a plastic producer), and 8 coloured large microplastic fragments sampled from the environment.

## 2.2 Real samples

Five samples collected through the French RNS-mP-P on 5 different monitoring beaches along the French Atlantic coastline, geographically distributed and representing different environmental contexts, were selected for the study. The monitoring sites considered are presented on Figure 2. Samplings were conducted in accordance with the EU methodology for monitoring mesolitter fragments and plastic pellets (MSFD TG-ML, 2023), except that all large microplastics were sampled, not only pellets, as detailed in CEDRE (2024). The dates of collection of the different samples are presented in Table 1.



Figure 2 : Location of the 5 monitoring beaches considered in the study



**Table 1 : List of the samples considered in the study. The name of the sample is the name of the monitoring beach where it was collected.**

Samples name	Date of sampling
Le Mont Saint-Frieux (62)	01.27.2025
La Grandville (22)	14.10.2024
Le Stang (29)	01.21.2025
La Baie de Gatteau (17)	01.15.2025
La Maison de Grave (33)	01.13.2025

### 2.3 Pre-treatment and visual analysis of the samples

In accordance with the EU methodology for monitoring mesolitter fragments and plastic pellets (MSFD TG-ML, 2023) and as detailed in CEDRE (2024), RNS-mP-P samples have been dried, treated to remove the organic matter, vegetation, and remaining sediment, and analysed, as part of the routine RNS-mP-P procedure. The analysis consisted in separating the mesoplastic fragments and the large microplastics, then sorting each category into different sub-categories, and finally counting the number of particles and weighing each subcategory (Figure 3). In the present study, only the large microplastic fraction was considered. For the large microplastics, the sub-categories considered are plastic pellets, biobeads, fibers, films, foamed polystyrenes, others foams and other plastic fragments.



**Figure 3 : Manual sorting of a RNS-mP-P sample prior to visual counting ©CEDRE**

The number of large microplastics particles per sample and per subcategory obtained by visual counting, are detailed in the Table 2.



Table 2 : Numbers of large microplastics in the real samples, obtained with the visual counting method

Samples	Plastic Pellets	Biobeads	Fibers	Plastic films	Other foams	Expended Polystyrenes	Other plastic Fragment	Total
Le Mont Saint-Frieux	55	32	0	0	0	37	7	131
La Grandville	28	0	0	0	0	1	6	35
Le Stang	14	0	0	0	0	0	23	37
La Baie de Gauseau	2	0	0	0	0	0	3	5
La Maison de Grave	9	0	0	0	0	11	2	22

## 2.4 Test of image analysis techniques

### 2.4.1 Photo acquisition

For the photo acquisition, each sample was placed on a coloured sheet (red, pale pink or turquoise), which was itself positioned inside a homemade camera stand device which was designed to ensure a repeatable photo acquisition (Figure 4). Indeed, during preliminary testing, the lack of precise repeatability in shooting height and angle resulted in significant issues, including unintended tilting of the camera, leading to reflections that were misidentified as additional particles, and apparent variations in particle size due to inconsistent shooting heights. The camera stand device was specifically designed to mitigate these issues, enabling precise control of the shooting height while ensuring the camera remains level. The stand offers adjustable height settings between 15 cm and 40 cm, features a stable base (adjustable from 20×20 cm to 40×40 cm), and is equipped with a thin upper platform to minimize shadowing effects. In addition, a built-in spirit level on the upper platform ensures proper camera alignment, thus minimizing the risk of unwanted reflections. This system is designed to enhance the repeatability and reliability of image acquisition, ensuring more accurate and consistent analytical results. Furthermore, to regulate light intensity and provide uniform illumination, a compact photo studio with integrated lighting was incorporated into the setup.

All photographs were taken under identical conditions (except for the background coloured-sheet that was changed) and standardised camera settings.

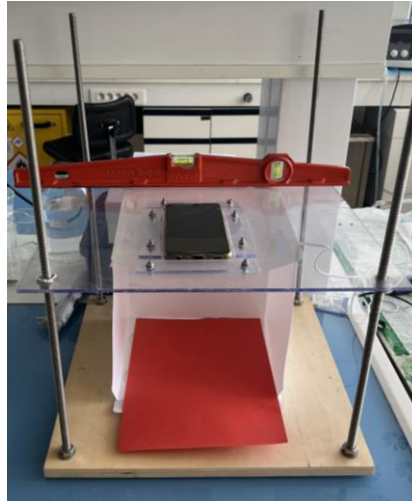


Figure 4: Homemade camera stand device developed by CEDRE to take the photographs  
©CEDRE

### 2.4.2 Test of ImageJ

#### *Software presentation*

**ImageJ** (Schneider et al., 2012) is an open-source software platform specialised in image processing and analysis, extensively employed in scientific research. It offers a comprehensive suite of tools for image enhancement, including filtering, segmentation, and contrast adjustment. ImageJ supports a wide range of quantitative analyses, such as distance measurement, area calculation, and particle counting.

The software is highly extensible through a robust plugin architecture and supports macro scripting in various languages, including JavaScript and Python, allowing for workflow automation and the development of customised analysis tools. Furthermore, ImageJ is capable of processing multi-dimensional datasets, including image stacks and video sequences, making it a versatile tool for a wide array of applications.

#### *Image analysis protocol*

The image analysis protocol using ImageJ proposed by CEDRE for this study, consisted in analysing 2 parameters: circularity and sizes. These parameters allow to differentiate plastic pellets, which have a round-like shape, from other large microplastics. The different steps of the photo analysis protocol are detailed below and summarised in the Figure 5:

1. Open the image in ImageJ:  
File > Open... and select the image.
2. Convert the image to grayscale (if it is not already):  
Image > Type > 8-bit.





## Free LitterAT deliverable D.2.2.6 (WP2-A2-Task4)

### 3. Adjust the threshold to detect particles:

Image > Adjust > Threshold.

Use the sliders to set the threshold so that the particles are well isolated. Areas highlighted in red represent the detected particles. Once satisfied, click Apply.

### 4. Enhance particle detection (if necessary, when particles are poorly separated), using two complementary functions:

- Process > Binary > Dilate to expand the particles or Erode to shrink them.
- Process > Binary > Watershed to better separate touching particles.

### 5. Analyse particles:

Analyze > Analyze Particles...

In the dialog box:

- Size (pixels<sup>2</sup>): Specify the size range of the particles to be included in the analysis.  
(To include all particles regardless of size, set the range from 0 to a very large value, e.g., 0–Infinity).
- Circularity:
  - Leave the default range (0.00–1.00) if no shape filtering is applied.
  - Restrict the range to select only circular shapes if necessary.
- Check Display Results to show the results in a table.
- Check Show Outlines or Show Masks to visualize the detected particle contours.
- To measure and display additional parameters (e.g., mean size, area), check Include in the Results Table.

### 6. Interpret the results:

- A results window opens listing the detected particles.
- The total number of particles and individual measurements such as particle area is displayed.

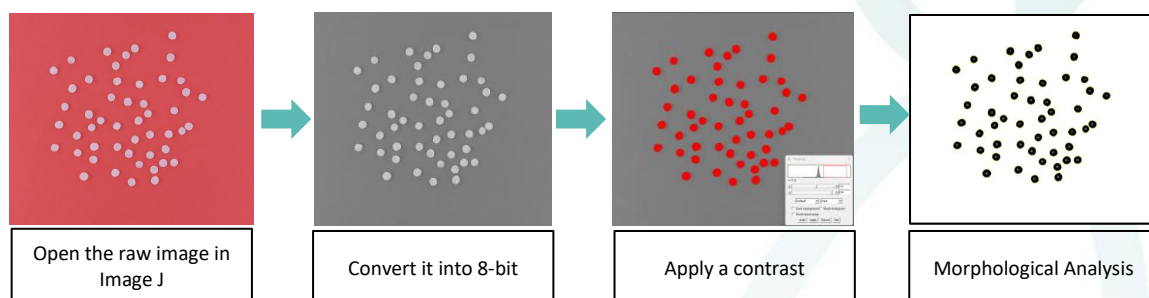


Figure 5 : The main steps of the image analysis protocol based on ImageJ





### 2.4.3 Test of PlugIm!

#### *Software presentation*

**PlugIm!** (Tan et al., 2018, [www.plugin.fr](http://www.plugin.fr)) is an open-source image analysis software developed by IFPEN. This software is specialised in image processing by using plugins. Around 120 plugins are available for different uses like filtering, analysis, segmentation or 3D interpretations. It provides a simple interface for the analysis of a large volume of data. PlugIm! became an open-source software in 2018, and is used in general by industries and the academic world.

#### *Image analysis protocol*

The image analysis protocol applied in this study uses 4 plugins that were selected among the 120 plugins available:

- The main plugin use for the particle analysis is the “**ARFBF morphological analysis**” plugin. It is a statistical model-based approach that involves Fractional Brownian Field (FBF) and 2D Autoregressive (AR) modelling. The approach consists in identifying the image background as an FBF, subtracting this background, and modelling the residuals by using the 2D AR approach.

Nevertheless, the use of this plugin needs filtering step to obtain a clear image for the analysis.

- “**The Edge preserving filter**” is used for the noise reduction on the image based on Schulze and Pearce work, providing a grayscale image by preserving the sharp edges of objects.
- “**3D Histogram automatic segmentation**” is an image segmentation algorithm used for the segmentation of the objects. Depending the picture this plugin uses different criteria of interest for the segmentation. The number of class of objects wanted can be modify.
- Finally, a final plugin is used to repeat the analysis for a defined number of pictures in a file. “**Batch processing**” is a plugin that automatises the operation by choosing the number of operations needed and by choosing a directory file for analysis. The Batch process gives all the steps off filtering and the export of the morphological analysis in a complete file for each picture.

As with Image J, an image processing protocol has been proposed by CEDRE for this study. The different steps of the photo analysis protocol are detailed below and summarised in Figure 6:

1. Open the file with images of interest  
Open the software and click on “File”-> Select the file with the images needed
2. Install Plugins



Open internet and go on: <https://www.plugin.fr/>

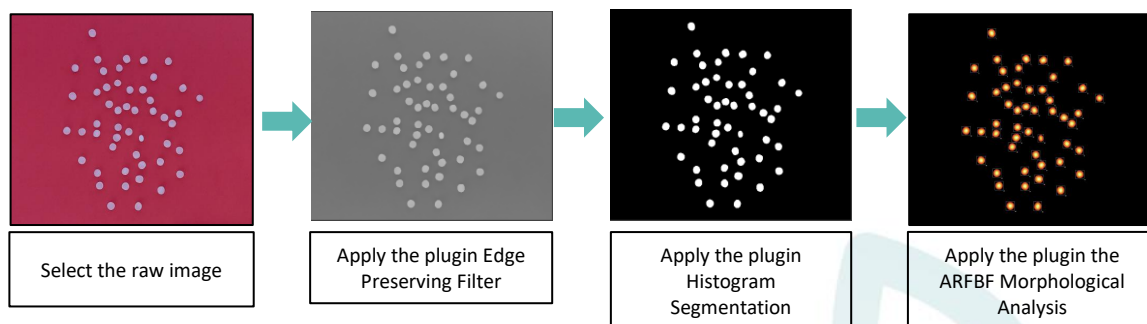
- Choose the plugins needed for the analysis in the open access list
- Download the plugins, a zip file is obtained.
- Open the zip file in plugin!

### 3. Method

- Run Batch Process and choose a directory file for the data export
- in batch process Select Edge Preserving Filter
- Then Select Histogram segmentation (Be sure that the criteria is on manual mode)
- Finally add the plugin Morphological analysis
- Click on Run the batch process and keep the software open during the analysis (Around 3 minutes for 5 pictures)

### 4. Data Export

- For each images a view of all the steps of analysis is available and a csv document gives the result of the morphological analysis.
- Different parameters appear in the export, the number of objects, the Area, Mean Radius, Standard deviation radius, minimum Radius, Maximum radius, LenghtEuc, LenghtGeo, Tortuosity, Elongation, Circularity and Perimeter.



**Figure 6 : The main steps of the image analysis protocol based on Plugin!**

The Plugin! software does not allow for a direct differentiation between pellets and fragments using its built-in tools. However, the export file generated following morphological analysis, could provide a sufficient data to distinguish particle types based on their circularity.

The result export file contains 12 morphological parameters (Table 3), all expressed in pixels.



**Table 3 : List of the parameters available in the PlugIn! export document for the last plugin “Morphological analysis”, with associated definition and purpose.**

Parameters	Definition	Purpose
<b>Number of objects detected</b>	Number of objects detecting on the image	Allow a fast counting of all the particles on the image
<b>Area (A)</b>	Total surface area of the object detected	Represent the size of the object
<b>Mean Radius (MR)</b>	Mean distance between the object's centre to its boundaries	Gives an idea of the overall size and regularity of the object
<b>Standard deviation radius</b>	Standard deviation of the distance from the object's centre to the boundaries	Measure the variability of the radius, indicate how regular or irregular the shape is.
<b>Min Radius/ Max Radius</b>	express the maximum and minimum radius from the centre to the boundaries of the object	Detect irregularities in the shape.
<b>Euclidean length (LengthEuc)</b>	Straight line distance between the two ends of an object	Baseline for comparing curves
<b>Geodesic length (LengthGeo)</b>	Actual length following the path of the object	More realistic measurement for curved objects
<b>Tortuosity</b>	Ratio of geodesic length to Euclidean length	Indicate how curved an object is, close to 1 straight, close to 0 tortuous
<b>Elongation (<math>LG^2/A</math>)</b>	Measure how stretched an object is based on geodesic length and area	Higher value indicates more elongated, thinner objects
<b>Elongation (<math>4 \times MR^2/A</math>)</b>	Variation of elongation using the mean radius instead of geodesic length	Alternative estimation of elongation based on radial shape
<b>Circularity (<math>4\pi A/P^2</math>)</b>	Shape descriptor that quantifies how close an object is to a perfect circle (1 = perfect circle)	Helps asses roundness and help for the differentiation between pellets and fragments
<b>Perimeter (P)</b>	Total length of the object's boundaries	Used for calculating other parameters and characterize edge complexity

### 3 Results

#### 3.1 Test of ImageJ

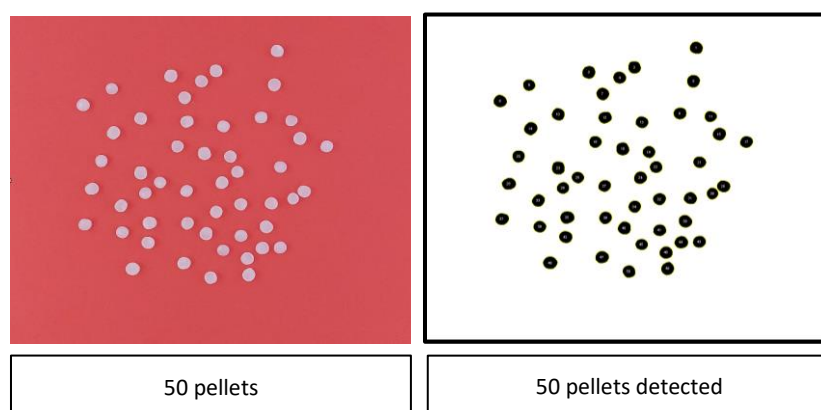
##### 3.1.1 Analysis of artificial samples

Before applying the ImageJ method to real samples, it has been first tested on artificial samples with the known compositions. Two artificial samples were used: the first containing 50 white pellets only (Figure 7), and the second containing the same 50 white pellets and 8 coloured plastic fragments (**Erreur ! Source du renvoi introuvable.**). The

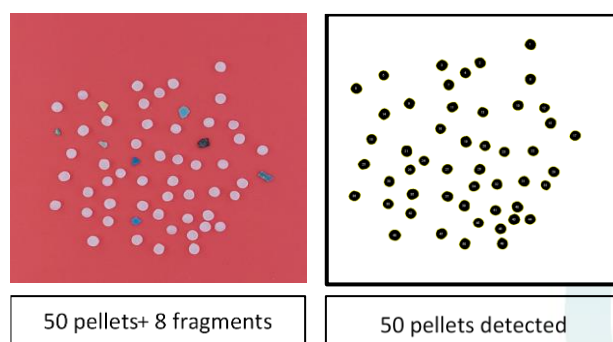


total duration of analysis for each sample, including image acquisition, file transfer, and processing using ImageJ, was approximately 10 minutes. The first test, performed on a red background to enhance contrast, enabled the detection of all 50 white pellets, yielding to a 100% detection rate.

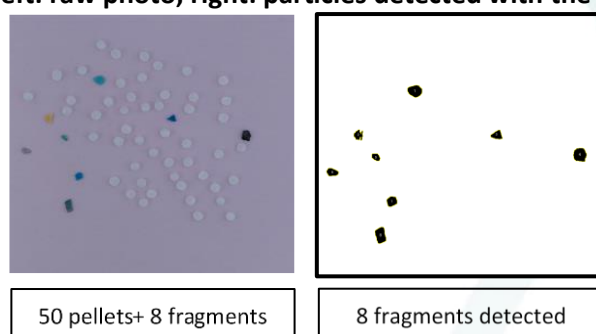
In the second test, also carried out initially on a red background, all 50 white pellets were again successfully detected. However, none of the coloured fragments were identified, likely due to insufficient contrast between their dark colours and the red background. When the same sample was analysed on a pale pink background, the improved contrast allowed for the detection of all 8 fragments but none of the pellets (Figure 9), indicating a double-step analysis was needed to identify all the particles.



**Figure 7 : Test 1 - analysis of artificial sample 1 (50 pellets) with a red background, (left: raw photo; right: particles detected with the ImageJ method)**



**Figure 8 : Test 2.A-analysis of artificial sample 2 (50 pellets + 8 fragments) with a red background (left: raw photo; right: particles detected with the ImageJ method)**





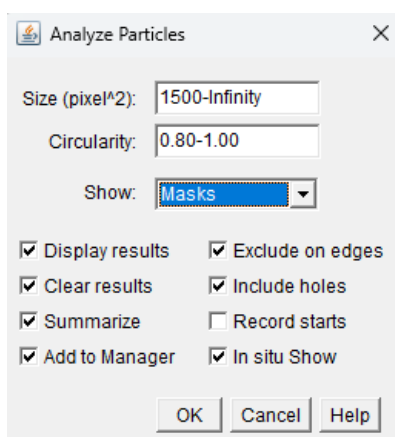


**Figure 9 : Test 2.B-analysis of artificial sample 2 (50 pellets + 8 fragments) with a pale pink background (left: raw photo; right: particles detected with the ImageJ method)**

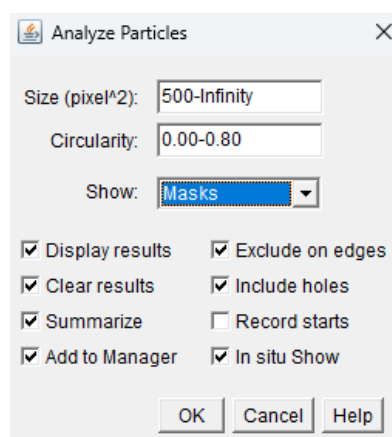
The parameters selected for the analysis of tests 1 and 2 containing pellets and fragments are described respectively in

Figure 10 and

Figure 11.



**Figure 10 : Parameters for the pellet analysis**



**Figure 11 : Parameters for the fragment analysis**

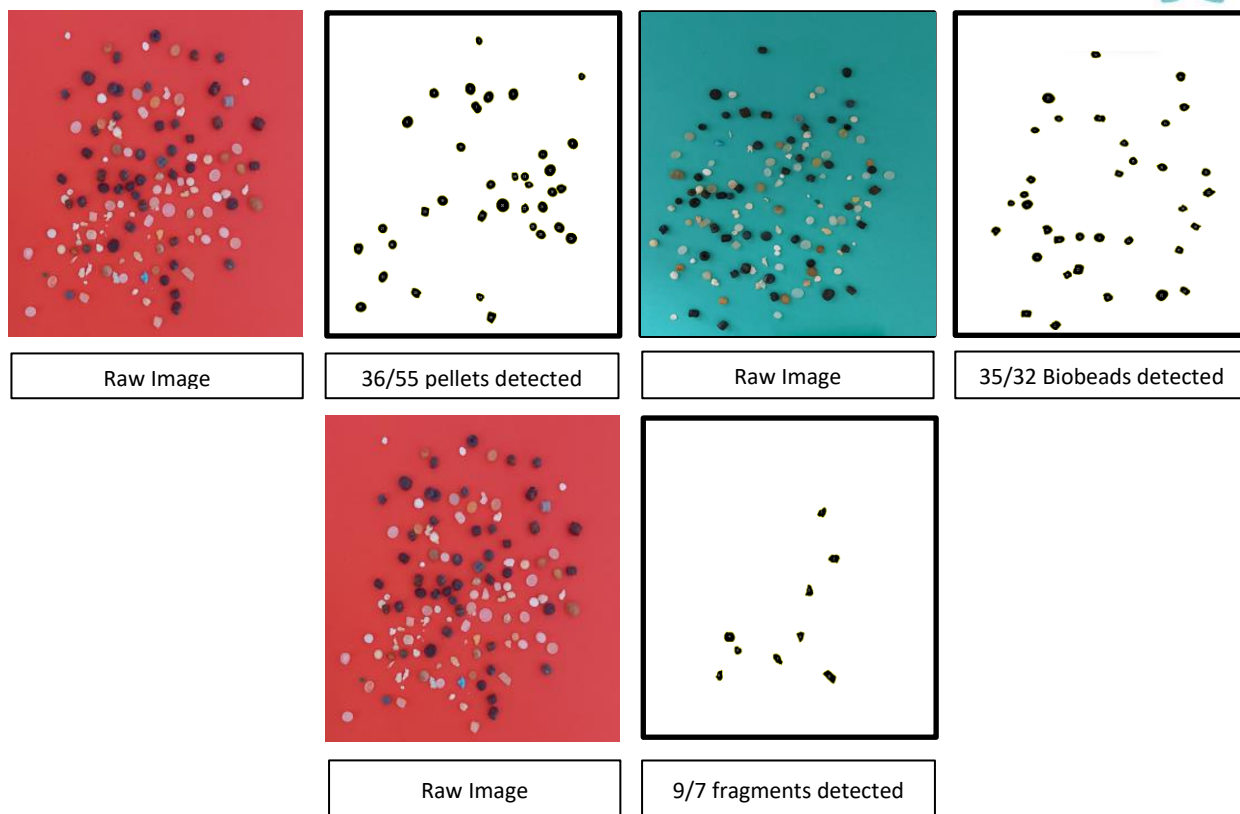
### 3.1.2 Analysis of real pre-treated samples

Following the analysis of artificial samples, the method was applied to the 5 real samples. For each pre-treated sample, a two-step analysis was conducted: one on a red background to identify white/clear particles, and another on a pale pink and/or turquoise background to improve coloured/dark particles detection. The results for each sample are presented below.

- Le Mont Saint Frieux (Neufchâtel-Hardelot, 62, France)

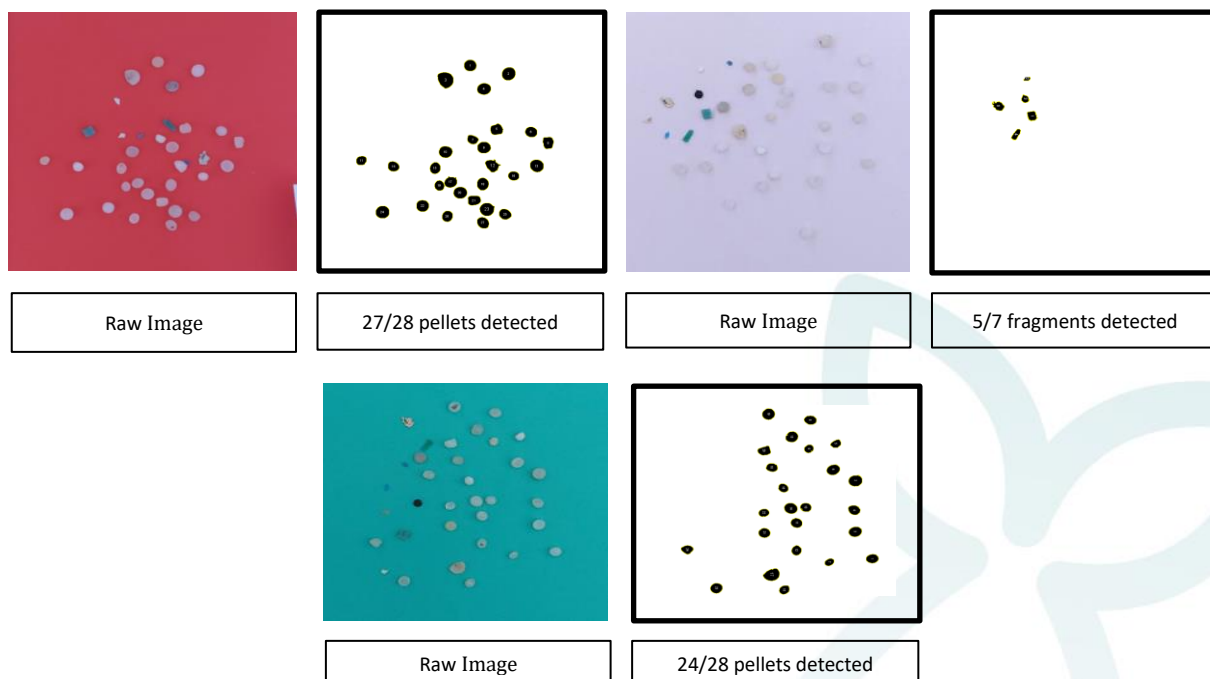
The sample "Le Mont Saint Frieux" (Figure 12) is the most complex of those analysed. It contains a wide range of particles, including 32 biobeads (used in certain wastewater treatment plants; Turner et al., 2019), 55 pellets, 7 fragments, and 41 expanded polystyrene (EPS) pieces. Due to their similar size and shape, biobeads and pellets can be difficult to distinguish visually, except that they have generally different colours (pellets being generally white whereas biobeads are generally black). In this sample, they were differentiated mainly based on this difference of colour. However, this colour-based differentiation is not universally reliable, as black pellets also exist. By adjusting the "Threshold" contrast setting, it was possible to effectively distinguish between the two in this specific case. Regarding the fragments, more were detected than expected as 2 pellets or biobeads were counted as fragments.





**Figure 12 : Results of the analysis of the sample Le Mont Saint Frieux (ImageJ)**

- La Grandville (Hillion, 22, France)



**Figure 13 : Results of the analysis of the Grandville sample (ImageJ)**

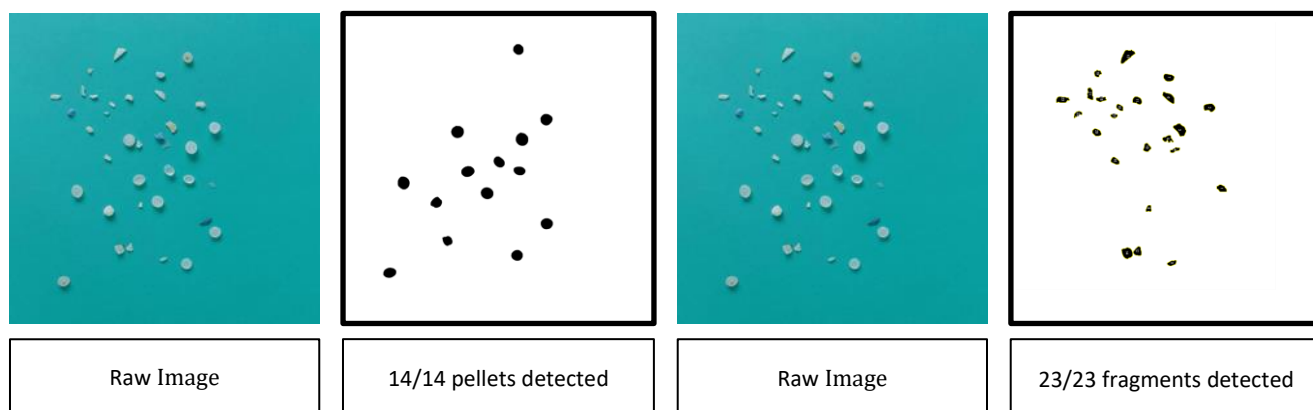
The sample “La Grandville” (Figure 13) contained 28 pellets, 6 fragments, and one piece of EPS. On a pink background, 27 of the 28 pellets were detected, compared to 24 on a



blue background. Regarding the fragments, 5 out of 7 were successfully identified on the pink background.

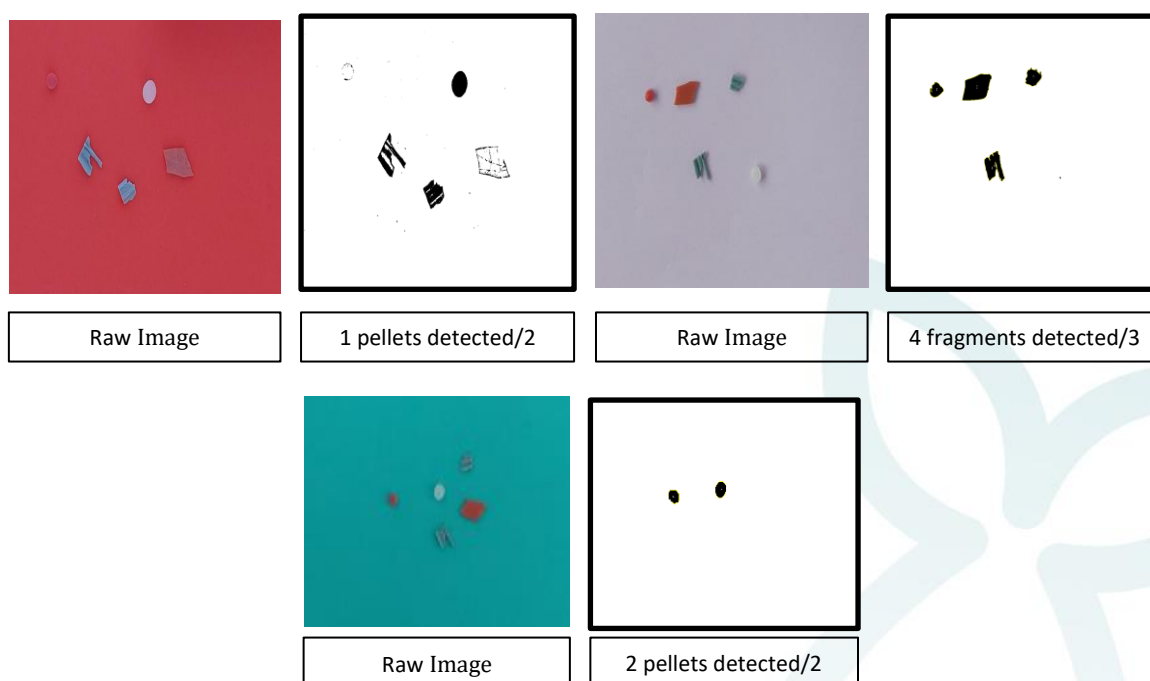
- Le Stang (St-Jean-Trolimon, 29, France)

The sample “Le Stang” (Figure 14) consists of 14 white pellets and 23 white fragments. An initial analysis on a red background enabled the detection of all 14 pellets, although not all fragments were identified. A subsequent analysis on a blue background achieved a 100% detection rate for both pellets and fragments.



**Figure 14 : Results of the analysis of the sample Le Stang (ImageJ)**

- La Baie de Gatseau (Saint-Trojan-les-Bains, 17, France)



**Figure 15 : Results of the analysis of the Baie de Gatseau sample (ImageJ)**

The sample “La Baie de Gatseau” is relatively small, composed of three coloured fragments and two pellets, one red and one white. With the red background, the white



pellet was easily identified but not the red one (Figure 15). Switching to a pink background allowed the detection of all three fragments but also counting the red pellet as a fragment. In addition, a blue background analysis enabled the identification of the two pellets based on their circularity parameters. However, this multi-step analysis led to double counting of several particles that were detected with different backgrounds.

- La Maison de Grave (Le Verdon-sur-Mer, 33, France)

The sample “La Maison de Grave” (Figure 16) presents an interesting case with 9 pellets (including one dark-coloured), 2 coloured fragments, and 11 expanded polystyrene (PS) particles. As with La Grandville sample, the method does not allow for clear differentiation between fragments and EPS particles, grouping them into a total of 11 fragments. On a red background, 8 of the 9 pellets were detected. On a blue background, 9 particles were initially classified as pellets; however, one was later identified as a fragment, bringing the actual pellet detection count back to 8, matching the result from the red background analysis.

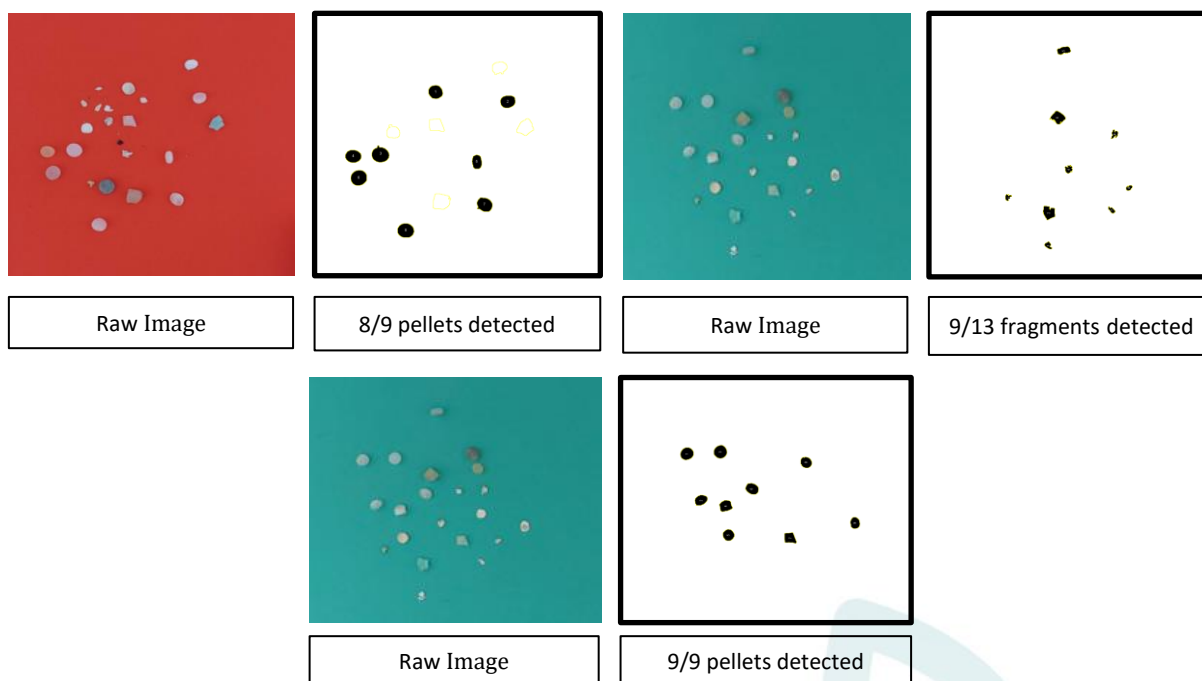


Figure 16 : Results of the analysis of La Maison de Grave sample (ImageJ)

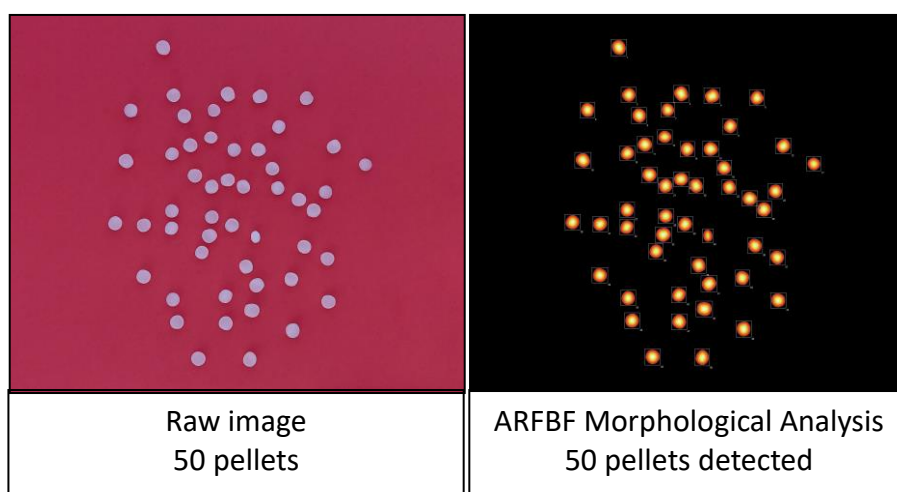
### 3.2 PlugIm!

#### 3.2.1 Analysis of artificial samples

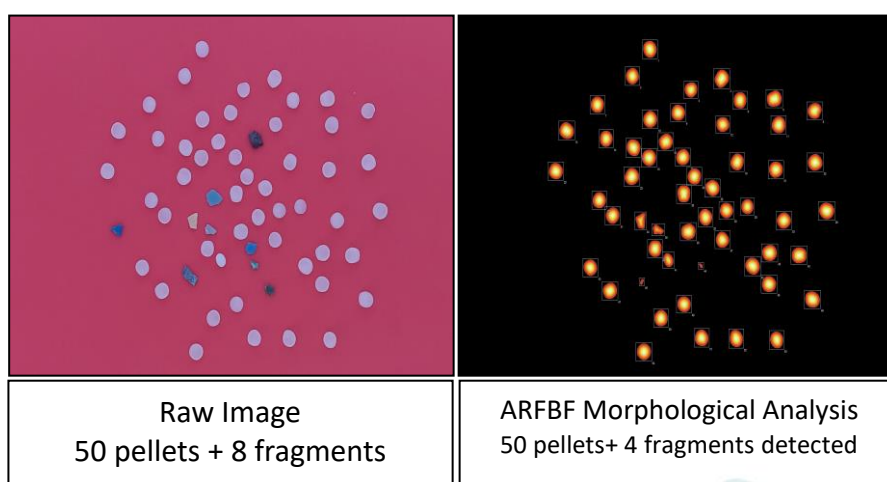
As with the ImageJ method, the analysis method using the PlugIm! tool was first tested on the artificial samples before being applied to the real RNS-mP-P samples. The same two artificial samples were used for this validation: one containing 50 white pellets (Figure 17), and another containing 50 white pellets and 8 coloured fragments (Figure 18). The complete analysis process (including image acquisition, file transfer, and automated processing in PlugIm!) was finished in approximately 10 minutes per sample.



For the PlugIm! method, only the red background was used as other backgrounds did not provide satisfying results.



**Figure 17 : Test 1 - analysis of artificial sample 1 (50 pellets) with a red background (left: raw photo; right: particles detected with the imagery method)**



**Figure 18 : Test 2-analysis of artificial sample 2 (50 pellets + 8 fragments) with a red background, (left: raw photo; right: particles detected with the imagery method)**

In the first test (Figure 17), all 50 pellets were successfully detected, demonstrating a 100% detection rate. In the second test (Figure 18), which included both pellets and fragments, 54 of the 58 particles were correctly identified. The five undetected particles were all fragments, likely due to insufficient contrast during the ARFBF morphological analysis phase.

These results underline the effectiveness of the method in detecting particles well contrasted. The variation in fragment colour, shape, and size appears to be the main factor influencing detection performance.





Table 4 : Detection rate for the artificial samples (red background)

Samples	Total particles in the sample	Total particles detected	Detection rate
Test 1: 50 white pellets	50	50	100 %
Test 2: 50 white pellets + 8 fragments	58	54	93 %

### 3.2.2 Analysis of real samples

PlugIm! was then applied to the 5 real samples collected on French Atlantic beaches. The analyses were carried out using the Batch Process plugin, with a total processing time of approximately 30 minutes for the 5 samples, including image acquisition, transfer, analysis, and data export.

- Le Mont Saint-Frieux (Neufchâtel-Hardelot, 62, France)

The sample “Le Mont Saint-Frieux” (Figure 19) presented the highest particle density and diversity. Many particles were either missed or incorrectly segmented due to their close proximity, which led to some being interpreted as single objects. In total, only 78 of the 131 particles were detected, resulting in the lowest detection rate (60%).

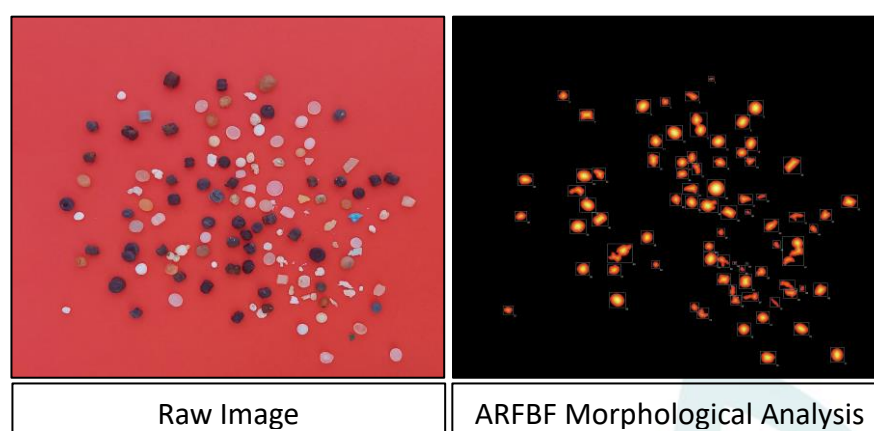
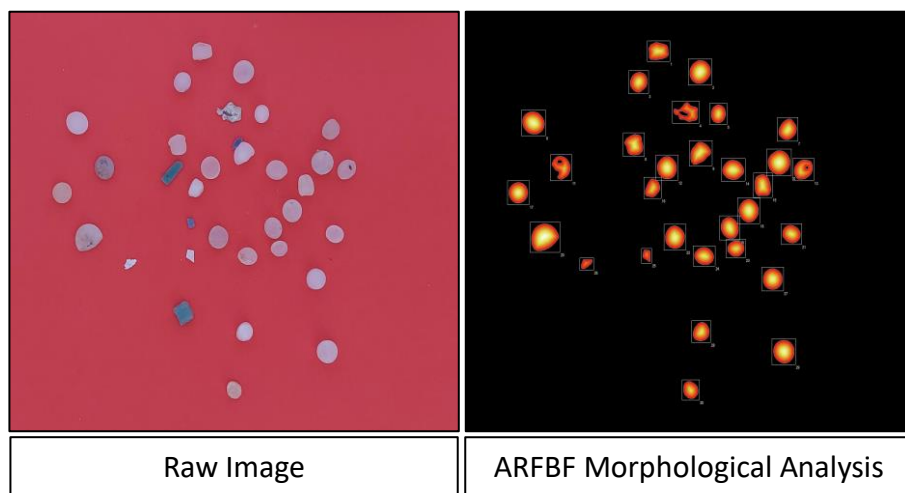


Figure 19 : Results of the analysis of the sample Le Mont Saint-Frieux (PlugIm!)

- La Grandville (Hillion, 22, France)

In the sample “La Grandville” (Figure 20), dark blue particles were not recognised by the system, likely due to contrast issues. Nonetheless, 30 of the 35 particles were detected, corresponding to an 86% detectability rate.

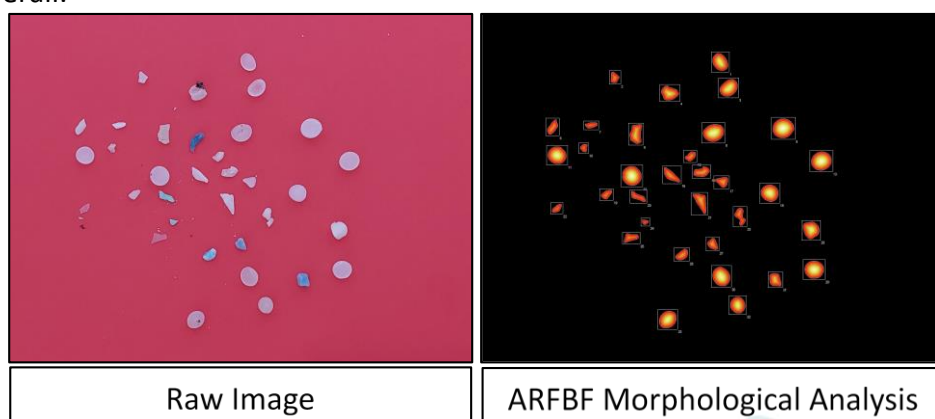




**Figure 20 : Results of the analysis of the sample La Grandville (PlugIm!)**

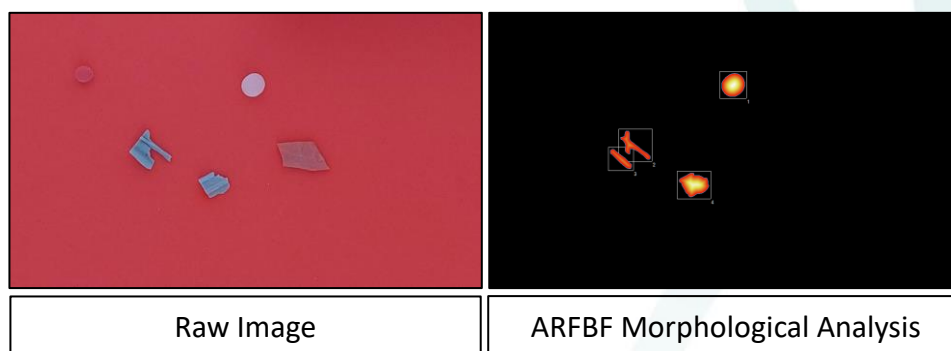
- Le Stang (St-Jean-Trolimon, 29, France)

In the sample “Le Stang” (Figure 21), 33 of the 37 particles were correctly identified, corresponding to an 89% detection rate. Despite the presence of dark-coloured particles, such as the red ones in the middle-left of the image, the method performed well overall.



**Figure 21 : Results of the analysis of the Stang sample (PlugIm!)**

- La Baie de Gatteau (Saint-Trojan-les-Bains, 17, France)



**Figure 22 : Results of the analysis of the sample La Baie de Gatteau (PlugIm!)**



As shown in Figure 22, the analysis of the sample “La Baie de Gatzseau” sample did not allow the detection of the two red particles which can be explained by the use of a red background. Additionally, one object was mistakenly segmented into two distinct particles by the morphological filter, impacting the total particle count. In total, 4 out of 5 particles were detected, yielding an 80% detection rate but including one double counting.

- La Maison de Grave (Le Verdon-sur-Mer, 33, France)

Figure 23 illustrates the results for the sample La Maison de Grave. The edge-preserving filter effectively removed noise from the image, enhancing clarity. However, one blue pellet was not identified in the final output. Overall, 21 out of 22 particles were successfully detected (96%).

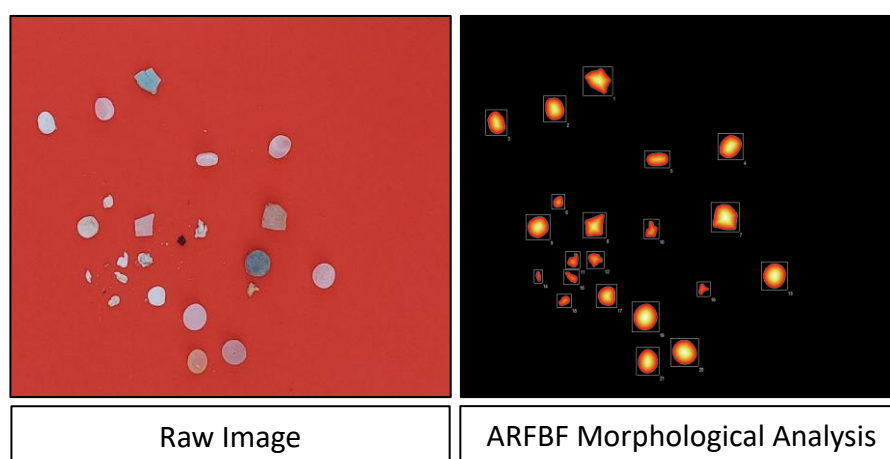


Figure 23 : Results of the analysis of the sample La Maison de Grave (Plugm!)

- Synthesis of the 5 samples

Table 5 illustrates the differences in detectability across samples. The lowest performance was observed for the sample Le Mont Saint-Frieux, likely due to particle crowding and visual complexity. The highest detection rate was achieved with the sample La Maison de Grave, though this may be partly attributed to its relatively low plastic concentration.

Table 5 : Detection rate for the real samples (red background)

Samples	Total particles detected	Total particles in the sample	Detection rate
Le Mont Saint-Frieux	78	131	60 %
La Grandville	30	35	86 %
Le Stang	33	37	89 %
La Baie de Gatzseau	4	5	80 %
La Maison de Grave	21	22	96 %



## 4 Discussion

In this study, the potential of traditional imagery tools to optimise the analysis of large microplastics samples in the context of a routine beach monitoring as recommended in MSFDTG-ML (2023), was tested using two different methods, one semi-automated based on the software ImageJ and one fully automated based on the software PlugIm!.

The original recommended method consists in visual sorting and counting whereas the alternative methods tested consists in taking photographs of pre-treated samples (cleaned to remove the organic matter) and analysing the photos with imagery softwares to detect the number of particles and their shape.

The two methods were tested on both artificial and real samples and results were compared with those obtained by visual counting. An overall comparison of the three methods based on different parameters, including pro&cons, is presented in Table 6.

**Table 6 : Comparison of different performance criteria for the tested methods**

Methods	Visual Counting	ImageJ method	PlugIm! method
<b>Type</b>	Original visual method	Semi-automated method with multisteps	Automated method with batch analysis
<b>Analysis Time</b>	~15–30 min/per sample	~5 min/photos but several photos could be necessary for one sample	~30 min/batch (5 samples)
<b>Reproducibility</b>	Moderate (operator-dependent)	Good	Excellent
<b>Capacity to distinguish particle types</b>	Good	Moderate	Low to moderate
<b>Confusion Risk (PS, biobeads)</b>	Low	Moderate	High
<b>Pro</b>	Reliability, detailed categorisation of particles	User control, could provide additional data such as particle sizes	Speed, batch processing, could provide additional data such as particle sizes
<b>Cons</b>	Time-consuming, operator dependant, only provide information about particle colour and number	Sensitive to contrast, time-consuming, risk of double counting when using different backgrounds for one sample	Object merging/risk of under counting



## 5 Conclusion

The study highlights the importance of the quality of the photos acquisition, with an appropriate background but also with particles well separated, to obtain relevant results. However, even with high quality photos, it appears that the imagery analysis performance is affected by the diversity of particles colours typically found in real samples, which decreases the ability to detect all the particles simultaneously with the tested methods and as a consequence, the results accuracy. This less affects pellets and biobeads that have generally a homogeneous colour, even if pellets can exhibit a wide range of colours and also undergo a colour evolution due to aging in the environment.

Results indicate that the semi-automated ImageJ method tested in the present study, can provide data that could meet the requirement of the EU-recommended protocol (which only considers the pellets in the large microplastic fraction) as the method is relatively performant to detect the pellets and can also distinguish them from other plastic particles like fragments (indicating no pre-sorting of the pellet in the sample is needed). However, it partially meets the requirement of the French monitoring program (that consider all large microplastic categories) although it is able to count a total number of particles and can also distinguished pellets from other particles types. However, this cannot be done without a multi-step analysis with analysis of several photos of the same sample, that needs to be processed by an operator which is time-consuming. In addition, this multistep analysis can lead to multiple detections of one particle, requiring a control and validation of the results by an operator which takes all the added value out of the approach. Thus, on the one hand, the method appears to have potential to optimise the EU-recommended methodology that only targets plastic pellets. This should be confirmed by additional testing on more samples (including samples with biobeads to ensure the ability to distinguish them from plastic pellets), in particular to assess the effect of pellet colours and aging on the capacity to robustly detect all the pellets. On the other hand, the method appears to have no added-value compared to the visual counting for the French monitoring program due to the time needed for processing, control, and validation.

Regarding the automated PlugIn! method, results indicated it could meet the requirement of the EU-recommended protocol, only if samples are pre-sorted to only retain pellets as the method is able to count a total number of particles without distinguishing the different particle subcategories. For this last reason, it only partially meets the requirement of the French monitoring program (that consider all large microplastic categories). However, further developments could optimise the particle detection. In addition, the possibility of batch analysis appears to be of great interest as it could allow to gain time for the operator and further work should be conducted to fine-tune the settings for this method to improve the particles detection.

In addition to the potential and limitations highlighted, it is important to mention that these methods can have potential in other contexts. For example, if an analysis of the particles size distribution is needed, both methods can provide precise morphological information on the detected particles. In addition, in the context of analysis of





homogenous samples (*e.g.* same shape and same colour) as it could be the case after an accidental release of plastic pellets at sea leading to important strandings on the coastline, the methods could allow a rapid counting of the number of particles if the method settings are selected appropriately (in particular with the batch analysis of the PlugIm! method).





## PART 2: Testing imagery coupled with a deep learning solution directly in the field

### 1 Presentation

Artificial intelligence (AI) is increasingly being applied to the identification and classification of macroplastics, particularly in waste sorting and recycling applications. Studies such as those by Wahab et al. (2006) and Scavino et al. (2009) have demonstrated the potential of AI in these fields. More recently, AI has been adopted for environmental applications, where it has been used to detect macroplastics in rivers (van Lieshout et al., 2020), on the ocean surface (de Vries et al., 2021; Moorton et al., 2021), and on beaches — for instance, through Ellipsis Earth's AI-based technology for litter mapping (<https://www.ellipsis.earth/educate-aboutus>).

In contrast to macroplastic research, AI applications for the detection and quantification of microplastics are still in their infancy. Traditional methods for quantifying microplastics, especially those targeting small particles (<1 mm), are time-consuming and involve several steps, including sampling, separating plastics from organic and mineral matter, and subsequent identification and quantification through chemical, visual, or physical methods. This process is not only costly and labor-intensive, but also heavily dependent on the operator, as the preparation and observation steps introduce variability in the results.

Current AI applications in microplastic research have mainly focused on image analysis. Advanced techniques such as FTIR, SEM, and holographic imaging have been used to identify microplastics, as demonstrated by the work of Zhu et al. (2021). Other studies, such as those by Gauci et al. (2019) and Cowger et al. (2020), rely on more traditional image analysis methods. More sophisticated AI approaches, such as the SMACC framework (Lorenzo-Navarro et al., 2018; 2020; 2021) and the research by Massarelli et al. (2021), use convolutional neural networks (CNNs) for microplastic identification. For example, the SMACC tool adapted the VGG-16 network (Simonyan & Zisserman, 2014) for this purpose, although its preliminary tests highlighted limitations due to insufficient data for training and validation. Moreover, most of these methods rely on pre-treated samples in which plastics have already been isolated, thereby eliminating the challenge of detecting microplastics among other particles and limiting their applicability in broader environmental and in situ contexts.

Despite these limitations, there are significant opportunities to improve the detection and quantification of microplastics through AI, particularly in environmental and



industrial settings. A pending patent (Rohais et al., 2022) was recently proposed by IFPEN to address these challenges. The resulting workflow has been tested in this study, to monitor large microplastics directly in the field on one of the Atlantic monitoring sites of the RNS-mP-P (Le Stang, Saint-Jean-Trolimon, Brittany, France).

## 2 Data and method

### 2.1 Photo acquisition – dataset

A photo acquisition protocol was established in 2023 and tested during the present study. The protocol involves taking photographs within quadrats in a standardised and repeatable manner to ensure consistency over time and space. Given that the concentration of meso- and microplastics is predominantly located along wrack lines on the coast, influenced by coastal processes, the photo acquisition was focused on these wrack lines. Taking benefits from protocol used in the context of the RNS-mP-P, the approach targeted a 100-meter-long strip along the wrack line(s). Two series of transects were conducted (Ta, Tb), capturing one photo every meter, resulting in a total of 101 photos per transect (Figure 24).

A survey site was selected in Brittany, France (Le Stang, Saint-Jean-Trolimon), where CEDRE has been conducting active monitoring since 2018. Data were collected between January 2023 and July 2024, with seasonal surveys yielding a comprehensive dataset of 2,169 measurements (Table 7).

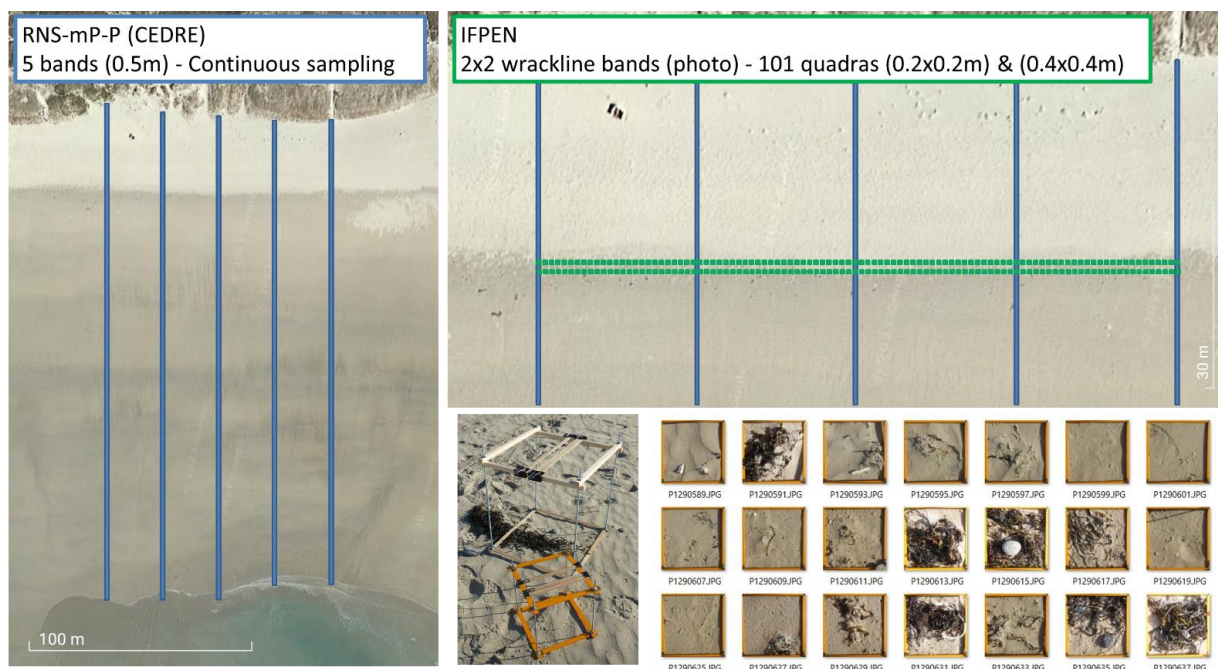
The acquisition time for one transect is about 15-20 minutes. The photos were acquired with a waterproof and shockproof NIKON CoolPix equipped with a GPS. The photos have a 1x1 RGB format with a dimension of 3456x3456 pixels. The photo size is about 4 to 5 MB.

**Table 7: List of the surveys and resulting dataset. Numbers of photo used for training and validating the artificial intelligence are listed (Tag for AI). To save time during the acquisition phase, a decision was taken to pass over photo during some surveys when no visible meso- or microplastics were observed**

Survey Nb.	Date	Location	Length (m)	Transect	Size (Quadrat)	Nb. Photo	Tag for AI	Visual counting	Comment
T1	01.10.2023	LE STANG	100	Ta	20x20	101	25	3	
T2	01.10.2023	LE STANG	100	Tb	20x20	100	100	3	1 No $\mu$ P
T3	04.18.2023	LE STANG	100	Ta	20x20	99	46	3	2 No $\mu$ P
T4	04f.18.2023	LE STANG	100	Tb	20x20	100	38	3	1 No $\mu$ P
T5	04.18.2023	LE STANG	100	Ta	40x40	29		3	Test
T6	04.18.2023	LE STANG	100	Tb	80x80	24		3	Test
T7	07.18.2023	LE STANG	100	Ta	20x20	101	26	3	
T8	07.18.2023	LE STANG	100	Tb	20x20	101	28	3	
T9	10.09.2023	LE STANG	100	Ta	20x20	84	31	3	17 No $\mu$ P
T10	10.09.2023	LE STANG	100	Tb	20x20	67	40	3	34 No $\mu$ P



T11	10.09.20 23	LE STANG	100	Ta	40x40	84		3	17 No $\mu$ P
T12	10.09.2023	LE STANG	100	Tb	40x40	67		3	34 No $\mu$ P
T13	01.23.2024	LE STANG	100	Ta	20x20	101	32	3	
T14	01.23.2024	LE STANG	100	Tb	20x20	101	22	3	
T15	01.23.2024	LE STANG	100	Ta	40x40	101		3	
T16	01.23.2024	LE STANG	100	Tb	40x40	101		3	
T17	04.23.2024	LE STANG	100	Ta	20x20	101		3	
T18	04.23.2024	LE STANG	100	Tb	20x20	101		3	
T19	04.23.2024	LE STANG	100	Ta	40x40	101		3	
T20	04.23.2024	LE STANG	100	Tb	40x40	101		3	
T21	07.10.2024	LE STANG	100	Ta	20x20	101		3	
T22	07.10.2024	LE STANG	100	Tb	20x20	101		3	
T23	07.10.2024	LE STANG	100	Ta	40x40	101		3	
T24	07.10.2024	LE STANG	100	Tb	40x40	101		3	
<b>TOTAL PHOTO IN 2023 &amp; 2024:</b>						<b>2169</b>	<b>388</b>		



**Figure 24:** The study site comprised a 100-meter stretch along the wrack line, examined using quadrats of 20x20 cm, 40x40 cm (and occasionally 80x80 cm), spaced at 1-meter intervals. Photos were captured using a dedicated device designed for consistent replication over time and space

## 2.2 Integrated workflow

The method implemented for this study is illustrated in Figure 25. It follows a relatively traditional workflow that begins with the data, in this case, the photos. The process involves (i) building the training database, (ii) training the artificial intelligence, and (iii) evaluating its performance against interpreted data. Beyond the identification and quantification of meso- and microplastics (abundance), the workflow incorporates an





additional step (iv) to convert abundances into mass using previously established correlation laws between morphological parameters and mass. Finally, the entire workflow is compared with results obtained by CEDRE within the framework of the protocol implemented for the RNS-mP-P, in line with EU recommendation (MSFD TG-ML, 2023). It should however be noted that the two approaches differ as the EU-recommended protocol consists in sampling over all the beach width, from the lowest wrackline to the back of the beach, providing a more integrative view of the pollution abundance on the beach.

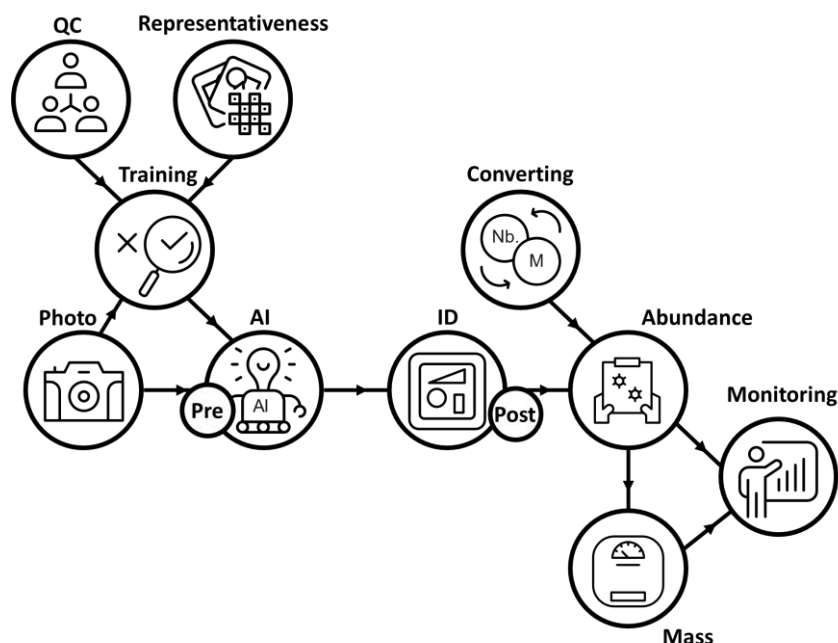
From a relative completion time perspective, the database preparation phase is likely the most time-consuming, requiring more than 50 days of work for quality control, labeling, and quantification. This phase is crucial, as the accuracy of the AI model depends on the quality and consistency of the training data.

In comparison, AI training and testing are performed over approximately 15-20 days, depending on the available computing capability. In this study, the IFPEN internal supercomputer was used to accelerate the process. While AI-based approaches significantly reduce the manual effort required for analysis, the initial investment in data preparation remains a major bottleneck in developing reliable and efficient machine-learning models for microplastic detection and classification.

### *2.2.1 Building the dataset for AI*

After the photo series were acquired, the first step was to create a training database for the AI. This process involved labeling the images to teach the AI how to identify meso- and microplastics. The categories chosen for labeling corresponded to the main categories used by CEDRE in the French national monitoring program for mesoplastics and large microplastics on beaches: pellets, fragments, fibers, films, and foams. Since the quality of the AI's performance relies heavily on the quality of the training dataset, a quality control (QC) phase was conducted. During this phase, three individuals—one experienced expert and two novices trained during the project—interpreted the entire dataset by performing classification and visual counts, resulting in a total of 6,825 measurements. The final dataset for AI training and validation included only the photos where all three interpreters proposed the same interpretation, ensuring a high-quality foundation for the learning process.

In addition to improving interpretation quality, the dataset of 6,825 measurements was also used to investigate representativeness. This analysis focused on assessing the impact of different photo acquisition strategies, such as taking photos every meter versus every five meters, and the use of different quadrat sizes, such as 20x20 cm versus 40x40 cm. These findings helped refine the photo acquisition protocol for more efficient and representative monitoring.



**Figure 25: The integrated workflow, developed by IFPEN as part of the Free LitterAT project, was designed to evaluate a deep learning solution aimed at supporting large microplastic and mesoplastic monitoring programmes**

### 2.2.2 Training strategy

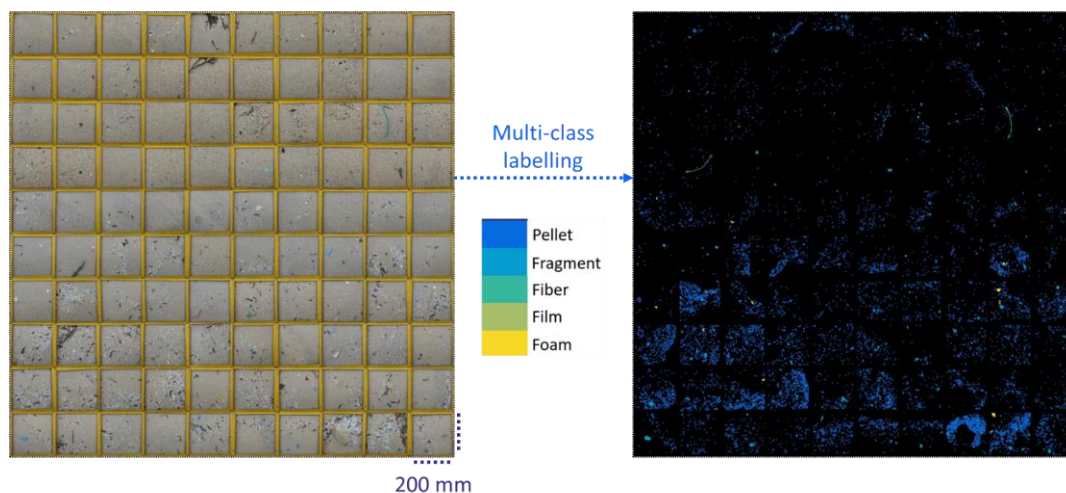
The training, validation, and testing of the AI were conducted in two phases. In the first phase, training data included all photos from survey 2 (T2) of the very first acquisition (10/01/2023) and 106 photos of synthetic samples prepared in advance (Synthetic). These synthetic samples contained known numbers and shapes of microplastics, evenly distributed to provide a balanced dataset. This initial version of the AI was then evaluated on data from surveys 3, 4, 13, and 14 to evaluate its performance. In the second phase, additional images from surveys 3, 4, 13, and 14 were added to the training data, alongside the original dataset. This allowed us to assess the impact of incorporating new information on the AI's predictive performance.

To optimize processing time and computational efficiency, the images were resized to 1280x1280 pixels before being fed into the AI. This resolution maintained sufficient detail for microplastic detection, with one pixel corresponding to 0.15625 mm, meaning that a 1 mm microplastic could be represented by more than six pixels. Additionally, pre-processing steps such as white balance normalization in the RGB channels were performed to ensure uniformity across all photos. The dataset was divided into three distinct subsets:

- Training photo: used to feed the model and extract key features from the images through the network architecture;
- Validation photo: used to fine-tune the model and calibrate it for accurate object recognition;



- Test photo: used in the final evaluation phase to assess the model's effectiveness. Importantly, these photos were never seen by the algorithm during the training or validation stages.

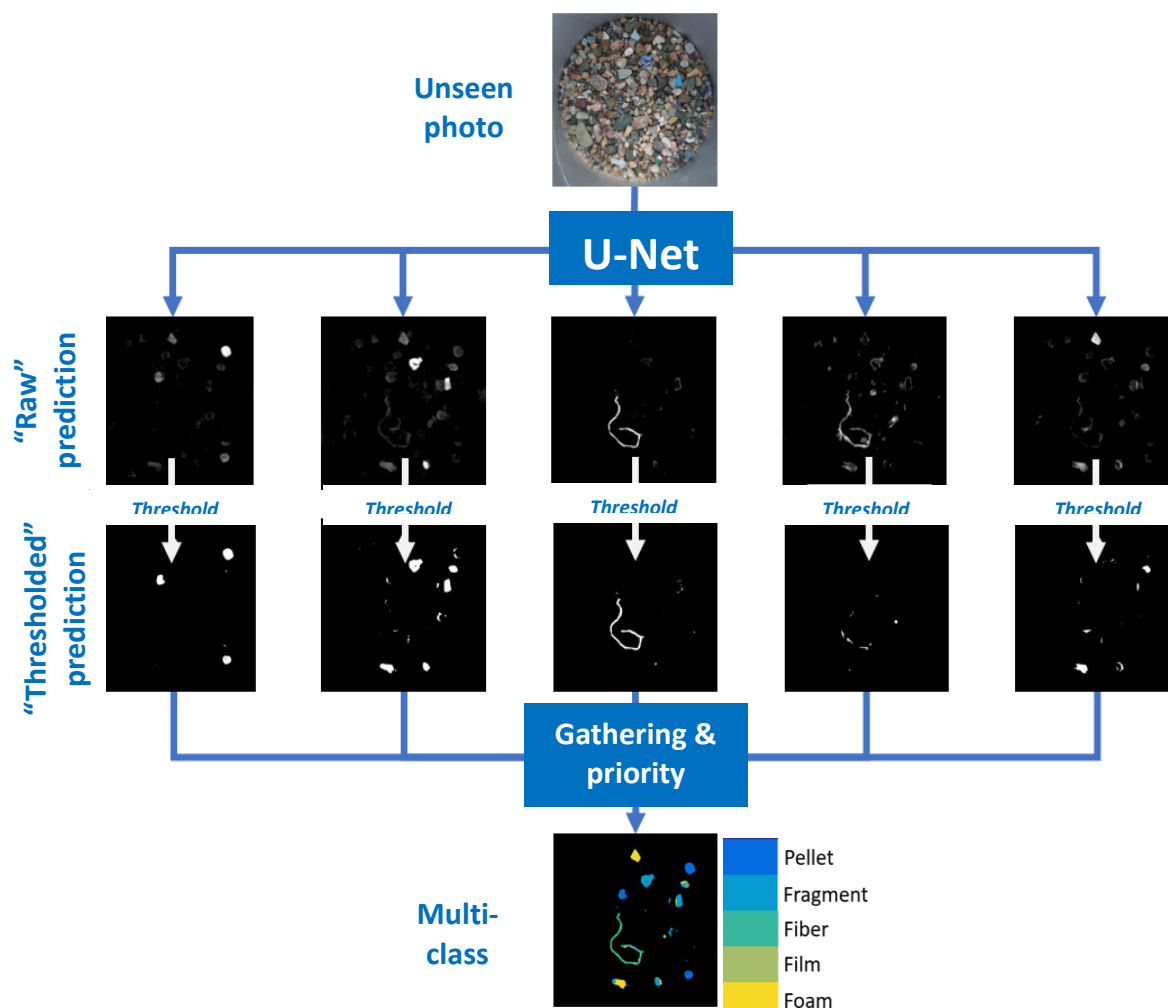


**Figure 26:** The full set of 100 photos from surveys T2 of the January 10, 2023, acquisition was labeled to create a high-quality training and validation dataset for the AI model. Each image was carefully analysed and classified into predefined categories (Pellets, Fragments, Foams, Films, and Fibers). This dataset serves as a critical foundation for training and validating the deep learning model

### 2.2.3 AI and inference

The AI model used in this study was the U-Net architecture developed by Ronneberger et al. (2015). The U-Net design features two symmetrical components: the down-sampling phase, which functions like a classic convolutional neural network to extract features while reducing the dimensionality of the input images, and the up-sampling phase, which restores the images' original dimensions and reconstructs them.

Inference involved applying the trained model to generate predictions for new, unseen images (e.g., test photos). The "raw" predictions produced grayscale images where each pixel was assigned a probability of plastic detection, ranging from 0 to 1 (Figure 27). Post-processing was then applied to convert these grayscale predictions into usable binary images. Using a predefined tolerance threshold of 0.7, the predictions were binarised, with pixels assigned a value of 0 (non-plastic) or 1 (plastic). In this project, U-Net was used in a multi-class configuration, and the post-processing step was applied separately to each of the five classes (pellets, fragments, foams, films, and fibers). This final process ensured that the predictions were accurate and interpretable for each category following priority rules from pellets to fibers.



**Figure 27:** U-Net is adapted to a multi-class configuration where the output layer contains multiple channels corresponding to different types of plastics (Pellets, Fragments, Fibers, Films, Foams). Each pixel in the segmented image is assigned a probability of belonging to one of these classes. Pixels are classified as plastic or non-plastic based on a probability threshold (e.g., 0.7). Multi-class prediction can then be used for morpho-math analysis and indicator quantification

### 2.2.4 Evaluation Metrics

The evaluation of the training process involves running predictions through the trained network on a dataset distinct from both the training and validation datasets but still part of the same overall dataset. The network's performance is quantified using the following two metrics: Precision and Recall. These metrics collectively ensure a robust assessment of the network's efficiency in identifying and classifying meso- and microplastics accurately.

Precision reflects the proportion of correctly identified plastics among all detected items. Precision measures the accuracy of detections and is defined as:





$$\text{Precision} = \frac{\text{True Positives}}{\text{True Positives} + \text{False Positives}}$$

Recall indicates the proportion of true plastics that were correctly detected by the network. Recall evaluates the network's ability to identify all true plastics and is defined as:

$$\text{Recall} = \frac{\text{True Positives}}{(\text{True Positives} + \text{False Negatives})(= \text{True Plastics})}$$

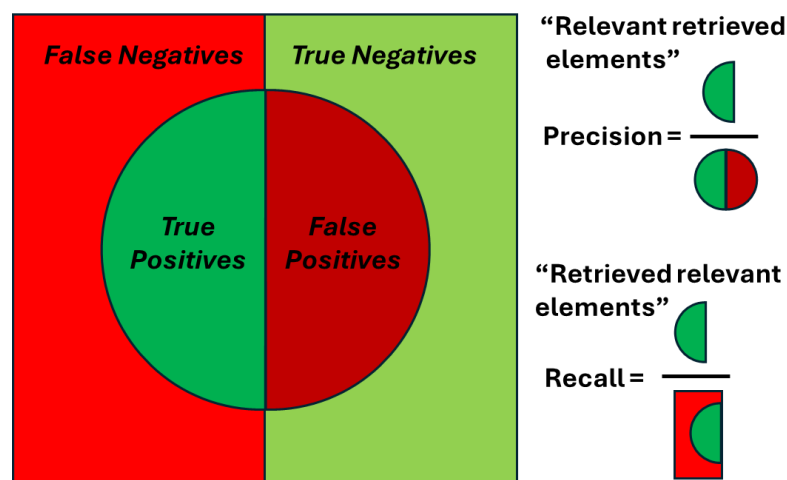


Figure 28: Evaluation metrics for machine learning used in the present study

### 2.2.5 Post-processing cut-off

A final post-processing step is applied to the images containing thresholded predictions to remove the smallest predicted microplastics. A cut-off threshold of 40 pixels is used, which corresponds to particles smaller than 1x1 mm. This ensures consistency with the categorization of large microplastics (1-5 mm) and mesoplastics (5-25 mm). By eliminating particles below this size threshold, the workflow focuses on the defined size ranges relevant for monitoring.

### 2.2.6 Abundance to mass conversion

The last stage of the workflow involves converting particle abundances into mass. This step is based on an internal IFPEN database that was used to calibrate five regression laws—one for each of the identified shapes (pellets, fragments, foams, films, and fibers). These regression laws were derived from synthetic samples, where the extracted 2D shapes and corresponding masses were precisely calibrated. Among the morphological parameters, the most relevant for mass estimation is the equivalent length, or Leq, defined as:

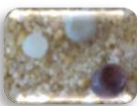

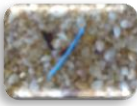


$$\text{Leq} = \sqrt{(\text{MaxDiameter} \times \text{MinDiameter})/4}$$



This parameter is used to establish a reliable relationship between particle size and mass using the following equation:

$$\log_{10}(Mass) = Slope \times \log_{10}(Leq) + Intercept$$

where Mass is defined in mg, Leq in mm, and Slope and Intercept are defined in Table 8 based on IFPEN database.

Table 8: Parameters used for the five categories on microplastic to convert the equivalent length (Leq in mm) into mass (mg). Number (Nb.) corresponds to the total number of measurements to constrain the regression laws					
	Class	Slope	Intercept	R <sup>2</sup> value	Nb.
	Pellet	2.05	0.76	0.85	231
	Fragment	2.60	-0.04	0.96	206
	Fiber	1.80	-0.21	0.23	64
	Film	1.99	-0.91	0.76	20
	Foam	2.39	-0.51	0.95	19

### 2.2.7 Comparison with official monitoring results

Finally, the results from the image analysis are compared to measurements performed on the same site and at the same time by CEDRE, in the context of the French national monitoring program for mesoplastics and large microplastics on beaches. This comparison allows for an evaluation of the differences between the sampling and extrapolation methods. It provides insights into the reliability and applicability of the workflow for monitoring large microplastics and mesoplastics on coastal environments, taking into account the EU-recommended methodology.



### 3 Results

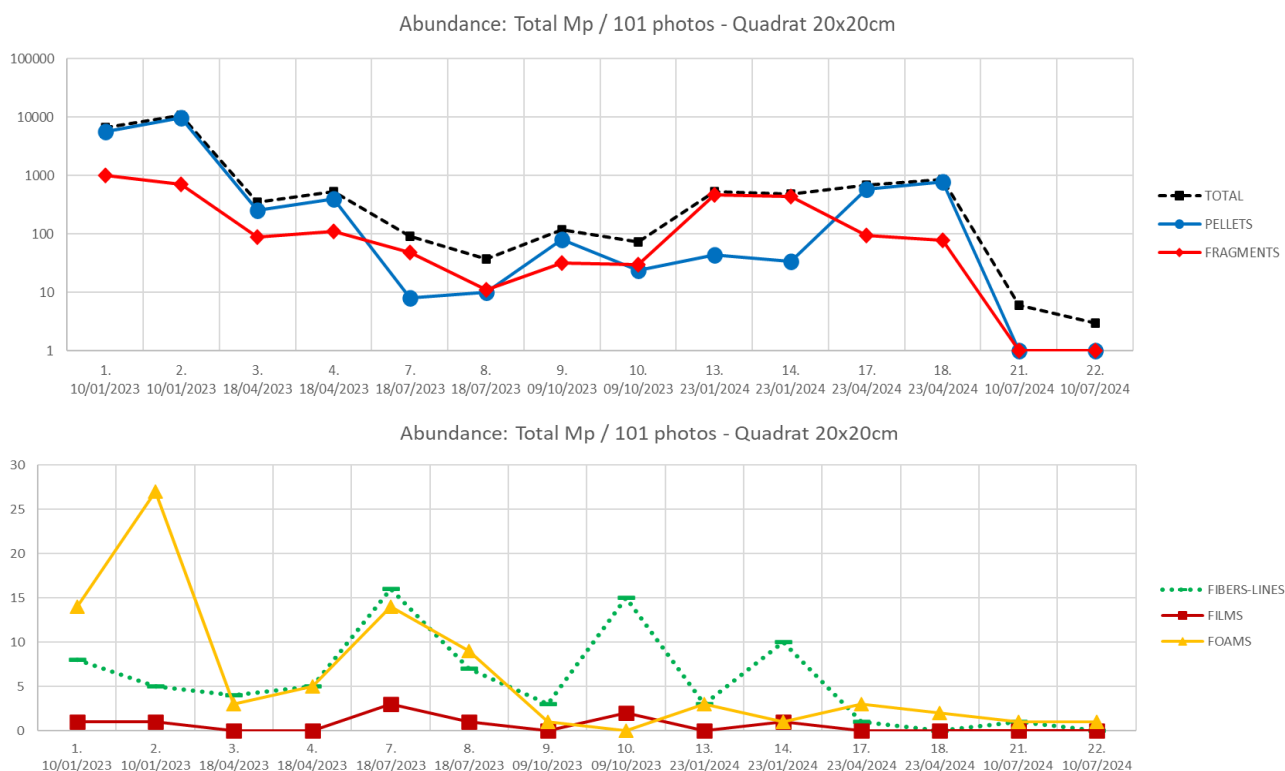
#### 3.1 Abundance of large microplastics and mesoplastics from photo

This section presents the quantified results of meso- and microplastic identification based on the photo interpretations conducted by the experienced operator. The variability in classifications between the experienced operator and novice operators 1 and 2 is analysed in detail in the discussion chapter, highlighting differences in detection accuracy, classification consistency, and the impact of training on operator performance.

Data acquisition was evaluated using quadrats of 20x20 cm, 40x40 cm, and 80x80 cm. However, the acquisition test with the largest quadrat (80x80 cm) was not replicated across multiple surveys due to the challenges associated with its size, making it difficult to implement effectively.

##### 3.1.1 Results for 20x20cm quadrats

The 20x20 cm quadrat photo surveys revealed significant temporal variability in microplastic distribution over the 1.5-year measurement period (Figure 29). Conducting paired surveys (e.g., T1 & T2, T3 & T4) helped account for spatial variability, with generally comparable results between pairs, though some differences were observed, particularly for less common forms like fibers (Figure 29).



**Figure 29: Relative variations in microplastic abundance over time. Results of the 20x20 cm quadrat surveys, based on photo interpretation by the experienced operator, over a period of 1.5 years (January 2023–July 2024). Five major forms of microplastics, as well as their total sum are illustrated. To improve readability, the dominant microplastic forms—Pellets and Fragments—are displayed on a logarithmic scale. The values presented correspond to the total number of microplastics identified across the 101 photos of each transect.**

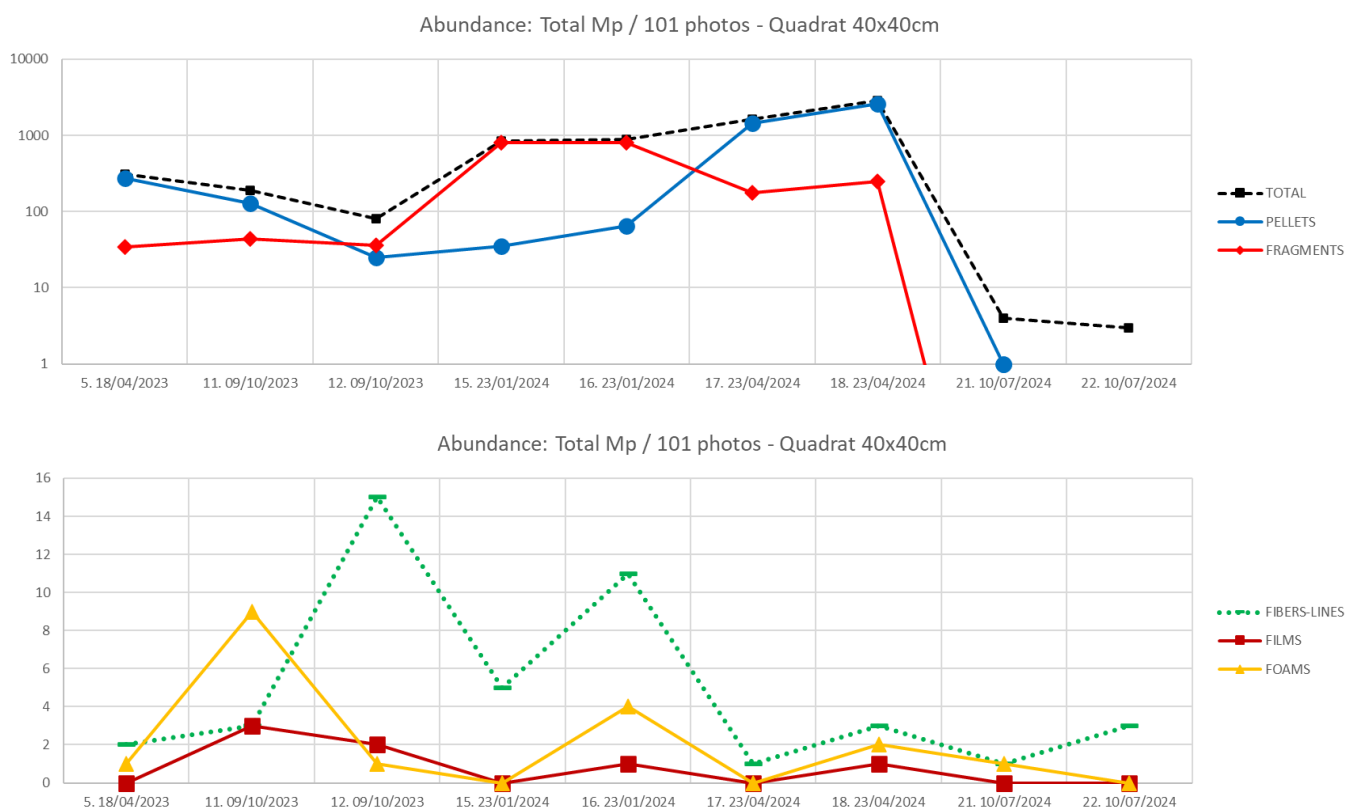


The highest microplastic abundances were recorded on 10/01/2023 (T1 and T2), with 10,578 microplastics identified and classified in T2 across 101 photos. In contrast, the lowest abundances were observed on 10/07/2024 (T21, T22), with only 3 microplastics detected in the 101 photos of T22.

Pellets and fragments were consistently the dominant forms of microplastics. A notable exception was the 18/07/2023 (T7, T8) survey, where all microplastic forms appeared in relatively equal proportions (ranging from a few units to a few dozen). Films remained underrepresented throughout the study, typically numbering fewer than five per transect.

### 3.1.2 Results for 40x40cm quadrats

The surveys conducted using 40x40 cm quadrats are fewer than those using 20x20 cm quadrats (Figure 30). However, their interpretation reveals similar trends and patterns in microplastic distribution. The dominant forms—Pellets and Fragments—remain consistent, along with the relative proportions between different microplastic types (Figure 30).



**Figure 30: Relative variations in microplastic abundance over time (Nb. before date on the axis refer to transect number). Results of the 40x40 cm quadrat surveys, based on photo interpretation by the experienced operator, over a period of 1.2 years (April 2023–July 2024). Five major forms of microplastics, as well as their total sum are illustrated. To improve readability, the dominant microplastic forms—Pellets and Fragments—are displayed on a logarithmic scale. The values presented correspond to the total number of microplastics identified across the 101 photos of each transect**





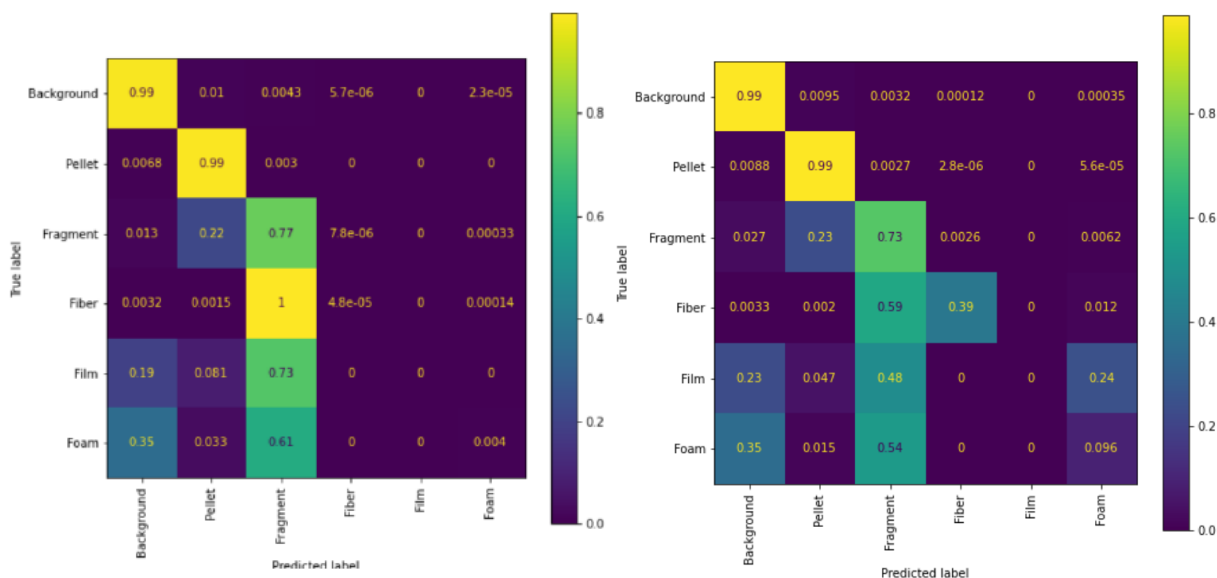
Interestingly, the total counts of microplastics from 40x40 cm quadrat surveys are not significantly higher than those from the 20x20 cm quadrats (Figure 30). Theoretically, given the fourfold increase in surface area, one would expect approximately four times more microplastics in the 40x40 cm surveys. However, the observed ratio is closer to 1:3, which could be explained by the heterogeneity of the particles deposition which are concentrated in the wracklines.

## 3.2 Deep learning solution evaluation

### 3.2.1 Training steps

A limitation of the initial training dataset was identified when using only the data from survey 2 (T2, 101 photos). This T2 dataset contained few or no instances of certain microplastic forms, such as fibers, films, and foams, leading to poor model performance in distinguishing these categories (Figure 31). To address this, the training dataset was expanded to include 106 additional photos from controlled synthetic samples (Synthetic), where all microplastic forms were evenly represented.

This augmentation significantly improved the model's ability to identify fibers and foams, which were initially often misclassified as fragments (Figure 31). However, the classification of films remained problematic, with a persistent tendency for misclassification as fragments. This issue suggests that further refinement is needed, possibly through additional labeled data.

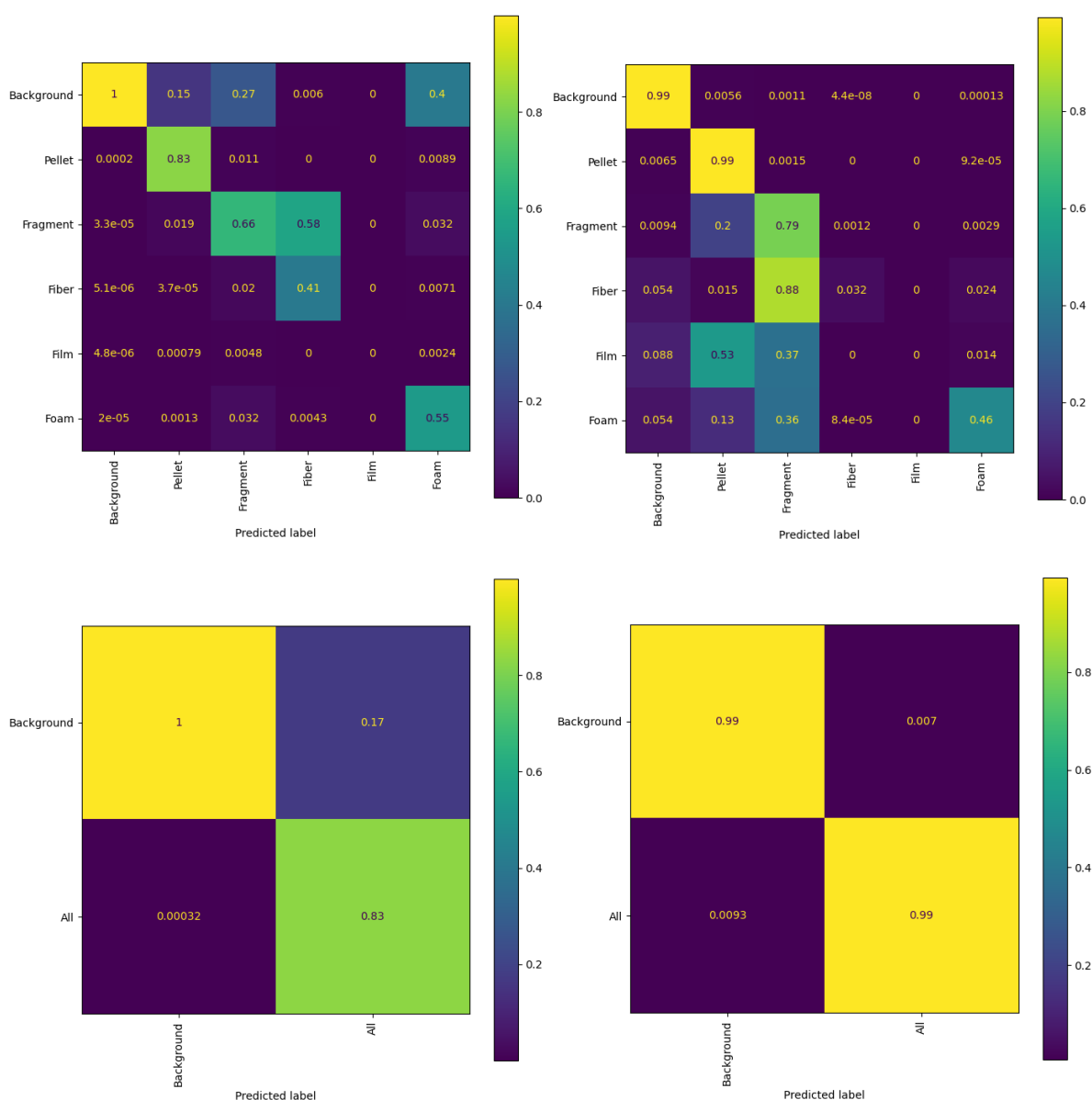


**Figure 31: Normalised confusion matrices (Recall) illustrating the improvement of training for shapes such as fibers and foams by completing the training base initially composed of survey 2 (T2) of 10/01/2023 (left) with additional photos of balanced synthetic samples (right). Yellow colours indicate good scores close to 1, dark blue ones indicate bad scores. The background of the images is always very well differentiated from the rest of the plastics**

The progressive training of the AI significantly improved the model's performance while consistently using the same core training dataset (T2 + Synthetic). The final stage of training involved expanding the dataset by incorporating selected images from surveys T3, T4, T13, and T14 (Figure 32). This additional data helped refine the model's ability to generalize to new images with different acquisition conditions (sunlight, dry sand...).



The overall performance of the model in distinguishing microplastics (training step) from the sandy background was highly effective, achieving a Precision score of 0.83 and a Recall score of 0.99. However, the performance varied significantly across different microplastic classes. While the model exhibited strong detection capabilities for Pellets and Fragments, its accuracy was notably lower for other forms such as Foams, Films, and Fibers. This discrepancy suggests that additional targeted training, potentially with more diverse and high-quality labeled data for these specific categories, could further enhance the model's classification accuracy.

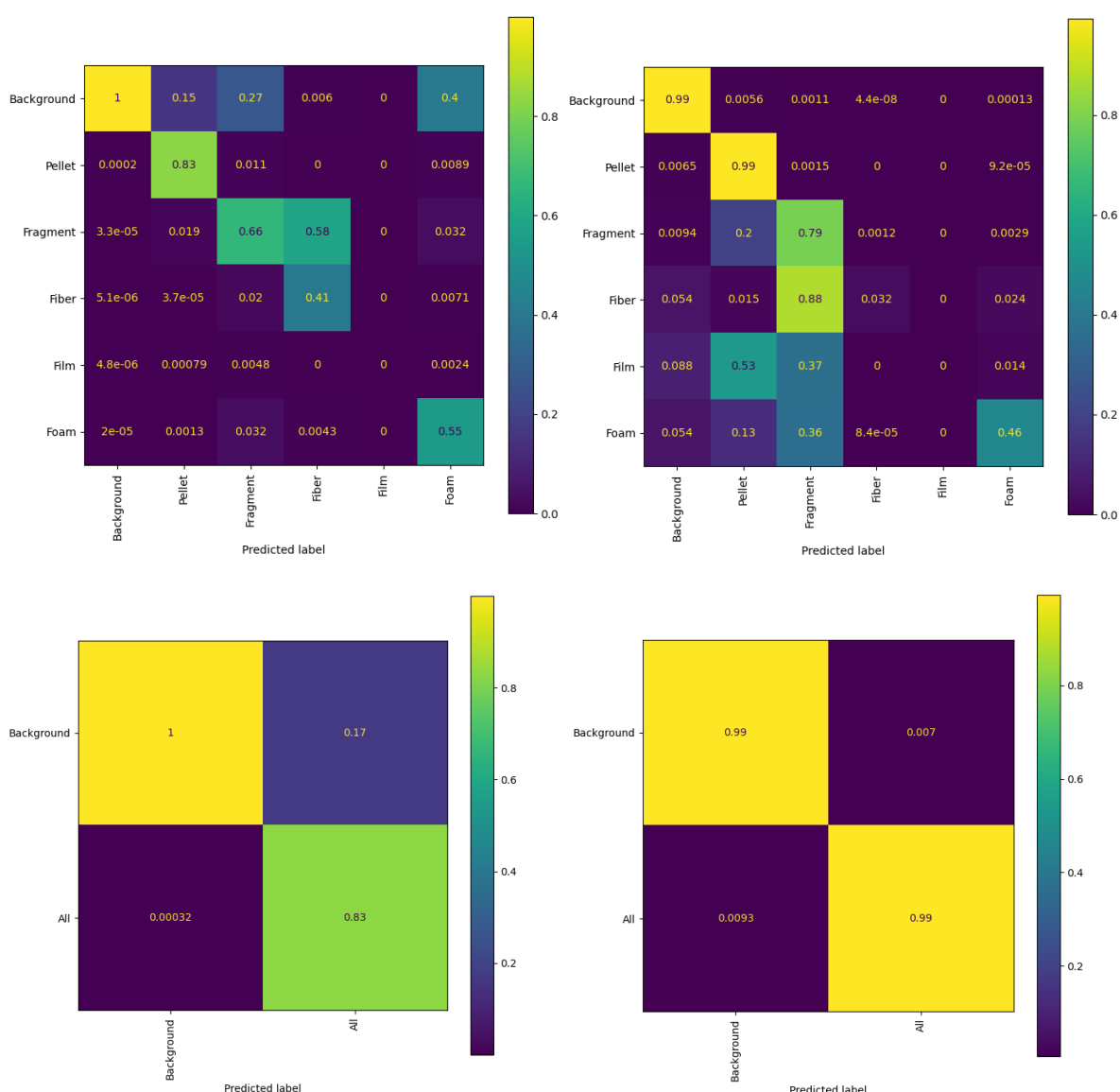


**Figure 32: Normalised confusion matrices for Precision (left) and Recall (right) during training phase using the most complete training database (T2 + Synthetic + Selection from T3, T4, T13 and T14). Uppermost matrices are detailed for the five categories of microplastics. Lowermost matrices illustrate the gathered results**



### 3.2.2 Validation steps

During validation, there were as many back-and-forth phases as for the training phase. Validation assesses a model's performance on unseen data during the training, helping detect overfitting. It ensures the model generalizes well and is not just memorizing the training data. The results for the validation align well with the findings from the training phase (Figure 33). However, precision and recall scores are slightly lower due to an increase in false positives, particularly with background elements being mistakenly classified as microplastics, including foams. Despite this, these issues should be considered with caution, as the overall proportion of fibers, films, and foams among the total microplastic count remains very low. More importantly, the model performs very well in distinguishing microplastics from the sandy background (Figure 33).

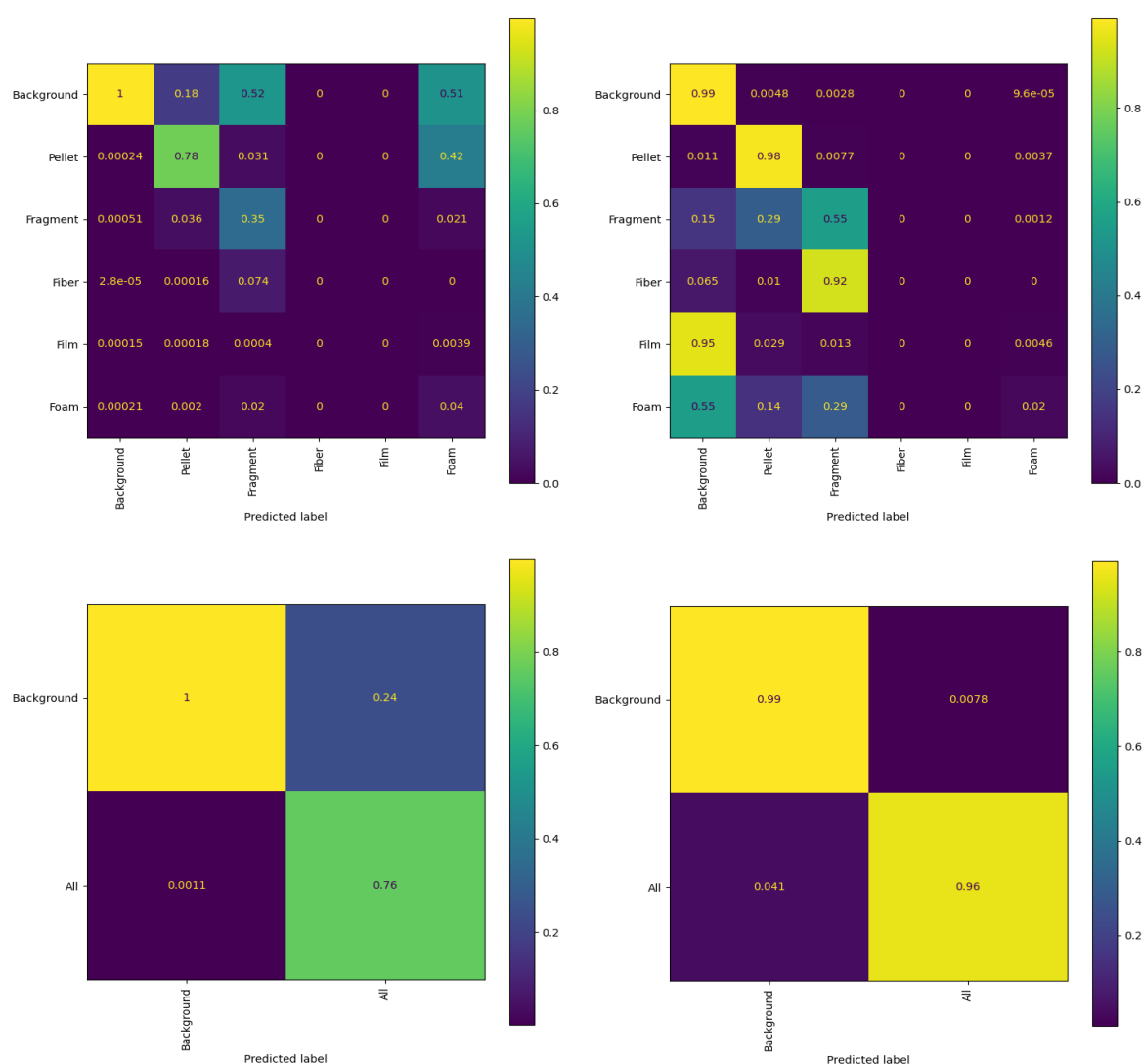


**Figure 33: Normalised confusion matrices for Precision (left) and Recall (right) during validation phase using the most complete training database (T2 + Synthetic + Selection from T3, T4, T13 and T14). Uppermost matrices are detailed for the five categories of microplastics. Lowermost matrices illustrate the gathered results.**



### 3.2.3 Test

The test dataset consists of 15 previously unseen photos, making its results crucial in evaluating the AI's ability to generalize and be deployed on a larger scale. The trends observed in the training and validation phases are reaffirmed. The AI performs exceptionally well in distinguishing microplastics from the sandy background, achieving a Precision of 0.87 and a Recall of 0.94. However, at the individual microplastic category level, films present the greatest challenge, often being misclassified as background, likely due to their transparent nature. Non-transparent films tend to be confused with fragments. Similarly, fibers and foams are categorised with moderate Precision and Recall, though the values remain reasonable. For pellets and fragments, the AI demonstrates strong performance, with Precision and Recall scores exceeding 0.9 for pellets and ranging between 0.4 to 0.7 for fragments (Figure 34).



**Figure 34: Normalised confusion matrices for Precision (left) and Recall (right) during test phase using the most complete training database (T2 + Synthetic + Selection from T3, T4, T13 and T14). Uppermost matrices are detailed for the five categories of microplastics. Lowermost matrices illustrate the gathered results.**





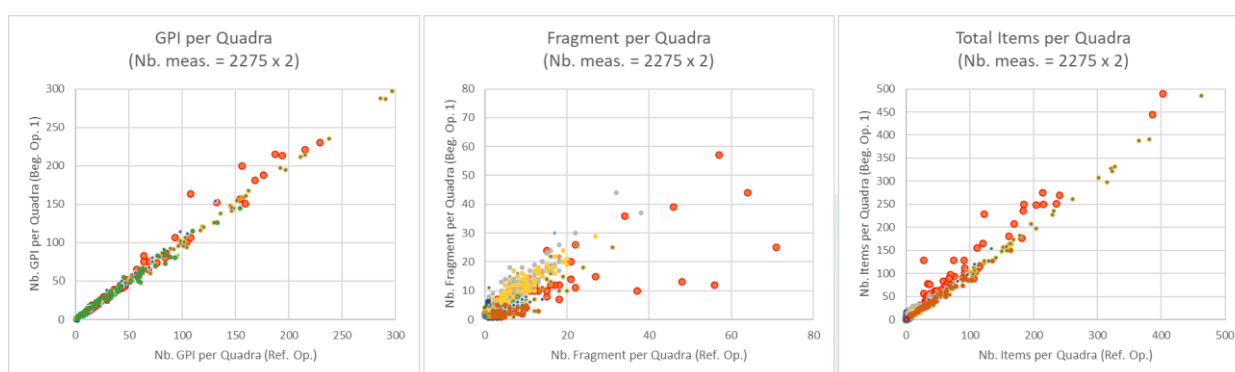
## 4 Discussion

### 4.1 Human factor

Building a high-quality training database is a crucial step in AI development, directly impacting its ability to make accurate predictions. The individuals responsible for labeling images play a key role in the overall workflow, as human perception can introduce biases.

To mitigate these biases, three operators independently interpreted the photos. Regular exchange meetings allowed for comparison of results and helped train novice operators. Over the course of a year, the two novice operators' identification and categorization results became increasingly aligned with those of an experienced operator (Figure 35). This is especially true for pellets and the total number of identified microplastics, where the agreement between operators is strong (Figure 35). However, for more challenging classes like foam and films, inconsistencies remain. These differences highlight the difficulty of accurately distinguishing certain microplastic forms, which can impact both human labeling and AI training. Further refinement in labeling protocols and additional training for operators may help reduce these discrepancies and improve overall model performance, specially by using synthetic and well controlled samples.

For AI training, only photos where all three operators reached a consensus were used for labeling. This approach aimed to minimize potential drift in human data interpretation. Such rigorous quality control is essential, not only for improving AI performance in this project but also for future expansions of the training dataset.



**Figure 35: Graphs illustrating the differences in microplastic identification and quantification (Pellet = GPI, Fragment and Total) between operator 1 and the experienced reference operator. Red colours indicate significant discrepancies, while green colours show better agreement. The dot size corresponds to the operators' training progression—larger dots represent early-stage assessments when the novices were less experienced, whereas smaller dots indicate improved accuracy as training progressed. A similar trend was observed for novice operator 2, reinforcing the importance of experience in accurately classifying microplastics**

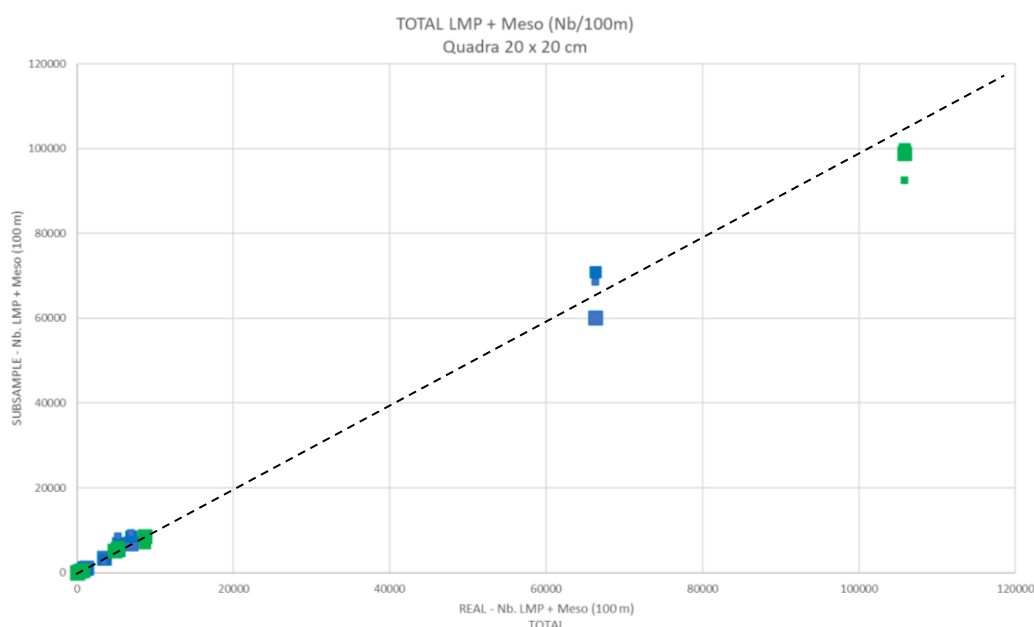


## 4.2 Database representativeness

To assess the representativeness of the database, we focused on the 20×20 cm quadrats, as they were the most numerous in our dataset. The project was structured around transects, with image acquisition conducted every meter along a 100-meter study area, resulting in a total of 101 photos per transect. To evaluate how subsampling would affect the dataset's ability to represent the full variability of the study area, we tested different subsampling strategies by selecting only (Figure 36):

- 1 out of every 2 photos (50% of the dataset);
- 1 out of every 5 photos (20% of the dataset);
- 1 out of every 10 photos (10% of the dataset).

This approach allowed us to determine whether a smaller dataset could still capture the same level of information as the full dataset, thus optimising data collection efforts while maintaining analytical reliability. A total of just 11 photos distributed across the 100-meter beach give a reasonable estimate of the total microplastic content (Figure 36). It highlights the potential for optimizing microplastic monitoring protocols without significantly compromising data quality. The finding that sub-sampling does not strongly impact the total microplastic estimates suggests that surveillance efforts could be streamlined. For professional monitoring networks, a 2 to 5-meter interval (resulting in 20 to 50 images per 100 m) strikes a balance between efficiency and accuracy. Meanwhile, for citizen-science initiatives, a 10-meter interval (11 images per 100 m) could provide a practical yet reliable approach for citizen-driven data collection.



**Figure 36: Total number of particles (LMP=Large Microplastics) quantified using subsamples was compared to the total number quantified using all 101 acquired photos. The largest squares represent cases where one photo out of every two was used in the analysis, while the smallest squares indicate cases where only one photo out of every ten was included. The blue points correspond to the first transect in each pair, such as Ta, while the green points correspond to the second transect in the pair, such as Tb**



### 4.3 AI performance and applicability

In the results section, the AI's performance was evaluated using traditional Precision and Recall metrics, derived from a pixel-by-pixel comparison between the initial image and the multi-class thresholded output from U-Net. However, monitoring programs such as the RNS-mP-P supervised by CEDRE typically assess microplastic (and mesoplastic) pollution through counts and mass measurements of particles or categories of particle. This section, therefore, discusses these figures and evaluates the AI's applicability in terms of real-world monitoring, *i.e.* at the scale of individual particles.

The AI's performance was tested in two stages, as outlined in the methodology. First, training, validation, and testing were conducted using only the survey T2 data (from 10/01/2023) along with synthetic samples. The AI was then applied directly to images from surveys T3, T4, T13, and T14, treating them as a new test series. The model's ability to generalise to these unseen images, which varied significantly in lighting, sand conditions (wet/dry), algae presence, sand grain size, shells, and pebbles, was low to relatively moderate.

In the second phase, the model was trained not only on the original dataset but also on a subset of images from surveys T3, T4, T13, and T14. This aimed to assess whether additional training data improved the AI's ability to accurately classify microplastics across different environmental conditions.

#### 4.3.1 Abundance

In the first training phase, the model performed exceptionally well, particularly in identifying Pellets and Fragments, with near-perfect accuracy for pellets. The total count of detected microplastics was also highly reliable. However, the AI tended to overestimate the number of microplastics present, relating to a surplus of false positives.

For less frequent categories such as fibers, films, and foam, the results were much more inconsistent. The AI struggled significantly with detecting films, often failing to identify them correctly. Fibers were either underrepresented or vastly overestimated, indicating difficulties in distinguishing them from other elements.

Despite these classification challenges, the overall detection performance was strong, with accuracy close to 100% for the total of microplastics. This confirms the AI's strong capability in differentiating microplastics from the sandy background. However, the misclassification issues suggest that while the model can effectively detect microplastics, it lacks precision in categorizing them correctly.

The second phase of testing, which involved directly transferring the AI's acquired knowledge to datasets partially used for training (T3, T4, T13, and T14), produced strong results in terms of abundance across training, validation, and test phases (Table 9). The detection of pellets was particularly high, with near-perfect relative performance (close



to 100%), though there was still an overestimation due to false positives. The total detected microplastic count was also overestimated, primarily because certain categories were misclassified, leading to misattributions between different microplastic types. This suggests that while the AI effectively differentiates microplastics from the sandy background, it struggles with precise categorisation, leading to a slight overestimation in the test series (104%).

**Table 9: Results of the microplastic abundance quantification for the reference set dedicated to training, based on the first step of the training strategy (Table A) and the second step including the enlarged training database with T2, Synthetic T3, T4, T13 and T14 photos (Table B)**

A. BASE (T2 - Synthetic)	AI								
	REAL	TRAINING		REAL	VALIDATION		REAL	TEST	
	Nb.	Nb. Iden.	Rel. Perf.	Nb.	Nb. Iden.	Rel. Perf.	Nb.	Nb. Iden.	Rel. Perf.
FIBER	17	5	29%	5	9	180%	1	6	600%
FILM	10	0	0%	5	0	0%	2	0	0%
FOAM	31	53	171%	14	10	71%	6	16	267%
FRAGMENT	360	416	116%	94	123	131%	89	109	122%
PELLET	7060	7048	100%	1459	1464	100%	1559	1575	101%
TOTAL	7478	7522	101%	1577	1606	102%	1657	1706	103%

B. BASE (T2 - Synthetic - T3, T4, T13, T14)	AI								
	REAL	TRAINING		REAL	VALIDATION		REAL	TEST	
	Nb.	Nb. Iden.	Rel. Perf.	Nb.	Nb. Iden.	Rel. Perf.	Nb.	Nb. Iden.	Rel. Perf.
FIBER	17	7	41%	5	0	0%	1	3	300%
FILM	10	0	0%	5	0	0%	2	0	0%
FOAM	31	98	316%	14	33	236%	6	7	117%
FRAGMENT	394	618	157%	109	259	238%	89	133	149%
PELLET	7084	7205	102%	1478	1595	108%	1567	1585	101%
TOTAL	7536	7928	105%	1611	1887	117%	1665	1728	104%

Interestingly, despite the addition of new training images, the classification performance was lower than in the initial training phase using only the T2 and Synthetic datasets. This counterintuitive result highlights an increased overestimation, particularly in the foam and fragment categories. Further refinements in post-processing, especially regarding the size of detected elements, could help mitigate these overestimations.

For the application of the AI on surveys T3, T4, T13, and T14, the results were less reliable, with a significant overestimation of microplastics. The AI correctly identified the absence of films, which aligns with the ground truth. However, it mistakenly predicted a high presence of foam, which was not actually present. This misclassification appears to stem from non-plastic environmental elements, such as algae and shell fragments, which were incorrectly categorised as foam. Additionally, both fragments and pellets were overestimated, leading to a total microplastic overestimation by approximately a factor of two.





The analysis of these transects revealed several environmental features—such as bird footprints, raindrops, bird eyes, and sand aggregates—that the AI may have confused with microplastics. These findings underscore the need for a more diverse and representative training dataset, particularly one that includes images containing ambiguous elements resembling microplastics. Expanding the dataset in this way would enhance the AI's ability to differentiate between true microplastics and similar-looking environmental features, improving its overall classification accuracy.

**Table 10: Results of the microplastic abundance quantification for the four tested transects, based on the first step of the training strategy (Table A) and the second step including the enlarged training database with T2, Synthetic T3, T4, T13 and T14 photos (Table B)**

A. BASE (T2 - Synthetic)	T3			T4			T13			T14		
	REAL	TEST		REAL	TEST		REAL	TEST		REAL	TEST	
	Nb.	Nb. Iden.	Rel. Perf.	Nb.	Nb. Iden.	Rel. Perf.	Nb.	Nb. Iden.	Rel. Perf.	Nb.	Nb. Iden.	Rel. Perf.
FIBER	0	0	NA	0	0	NA	1	10	1000%	4	8	200%
FILM	0	0	NA	0	0	NA	0	0	NA	0	0	NA
FOAM	0	63	NA	0	44	NA	0	117	NA	0	105	NA
FRAGMENT	17	83	488%	18	60	333%	123	606	493%	67	480	716%
PELLET	104	110	106%	125	123	98%	13	89	685%	4	71	1775%
TOTAL	121	256	212%	143	227	159%	137	822	600%	75	664	885%

B. BASE (T2 - Synthetic - T3, T4, T13, T14)	T3			T4			T13			T14		
	REAL	TEST		REAL	TEST		REAL	TEST		REAL	TEST	
	Nb.	Nb. Iden.	Rel. Perf.	Nb.	Nb. Iden.	Rel. Perf.	Nb.	Nb. Iden.	Rel. Perf.	Nb.	Nb. Iden.	Rel. Perf.
FIBER	0	0	NA	0	0	NA	1	7	700%	5	5	100%
FILM	0	0	NA	0	0	NA	0	0	NA	0	0	NA
FOAM	0	43	NA	0	22	NA	0	11	NA	0	12	NA
FRAGMENT	17	140	824%	15	84	560%	108	131	121%	37	83	224%
PELLET	90	109	121%	101	146	145%	8	42	525%	2	24	1200%
TOTAL	107	292	273%	116	252	217%	117	191	163%	44	124	282%

The AI trained with a small selection of photos from surveys T3, T4, T13, and T14 demonstrates significantly improved performance, with a fivefold increase in relative performance on surveys T13 and T14 (Table 10). This improvement is primarily due to a reduction in the overestimation of foams, related to fewer false positives. This outcome is encouraging, as it suggests that incorporating new photos that align with the tested series leads to substantial enhancements in prediction accuracy.

#### 4.3.2 Mass

The mass (mg) results follow the same trend as the abundance results. Interestingly, the validation and test training series from the first phase show a decline in relative performance when the selection of photos from T3, T4, T13, and T14 is added (Table



11). However, this addition leads to a significant improvement in relative performance for all the surveys T3, T4, T13 and T14 during the second phase (Table 12).

**Table 11: Results of the microplastic mass quantification for the reference set dedicated to training, based on the first step of the training strategy (Table A) and the second step including the enlarged training database with T2, Synthetic T3, T4, T13 and T14 photos (Table B)**

A. BASE (T2 - Synthetic)	AI								
	REAL	TRAINING		REAL	VALIDATION		REAL	TEST	
	Mass (mg)	Mass Est. (mg)	Rel. Perf.	Mass (mg)	Mass Est. (mg)	Rel. Perf.	Mass (mg)	Mass Est. (mg)	Rel. Perf.
FIBER	103	28	27%	31	51	164%	6	16	289%
FILM	45	0	0%	13		0%	8	0	0%
FOAM	204	550	269%	94	90	95%	43	177	414%
FRAGMENT	4639	5383	116%	1215	1600	132%	1149	1426	124%
PELLET	100760	101074	100%	20376	20704	102%	22337	22666	101%
TOTAL	105751	107035	101%	21730	22445	103%	23542	24285	103%

B. BASE (T2 - Synthetic - T3, T4, T13, T14)	AI								
	REAL	TRAINING		REAL	VALIDATION		REAL	TEST	
	Mass (mg)	Mass Est. (mg)	Rel. Perf.	Mass (mg)	Mass Est. (mg)	Rel. Perf.	Mass (mg)	Mass Est. (mg)	Rel. Perf.
FIBER	103	45	44%	31	0	0%	6	13	240%
FILM	45	0	0%	13	0	0%	8	0	0%
FOAM	204	1047	512%	94	368	391%	43	71	166%
FRAGMENT	5084	7983	157%	1411	3374	239%	1149	1697	148%
PELLET	101117	107451	106%	20611	23008	112%	22337	23833	107%
TOTAL	106554	116526	109%	22161	26749	121%	23542	25614	109%

Unlike the results in abundance, where the improvement in relative performance for surveys T3 and T4 was not significant despite the inclusion of additional training data from T3, T4, T13, and T14, the mass results exhibit a clear improvement in relative performance during the second training phase for the four surveys (T3, T4, T13, T14). These findings are highly encouraging and highlight the importance of monitoring both abundance and mass indicators, as the overall trends may differ between these two metrics.



**Table 12: Results of the microplastic abundance quantification for the four tested transects, based on the first step of the training strategy (Table A) and the second step including the enlarged training database with T2, Synthetic T3, T4, T13 and T14 photos (Table B)**

A. BASE (T2 - Synthetic)	T3			T4			T13			T14		
	REAL	TEST		REAL	TEST		REAL	TEST		REAL	TEST	
	Mass (mg)	Mass Est. (mg)	Rel. Perf.	Mass (mg)	Mass Est. (mg)	Rel. Perf.	Mass (mg)	Mass Est. (mg)	Rel. Perf.	Mass (mg)	Mass Est. (mg)	Rel. Perf.
FIBER	0	0	NA	0	0	NA	5	46	937%	16	47	284%
FILM	0	0	NA	0	0	NA	0	0	NA	0	0	NA
FOAM	0	628,7	NA	0	443	NA	0	1355	NA	0	1220	NA
FRAGMENT	176	1073	609%	230	7723	3356%	1605	7742	482%	878	6035	687%
PELLET	201	1423	708%	1819	1709	94%	162	764	472%	58	598	1024%
TOTAL	377	3124	829%	2049	9875	482%	1772	9907	559%	953	7899	829%
B. BASE (T2 - Synthetic - T3, T4, T13, T14)	T3			T4			T13			T14		
	REAL	TEST		REAL	TEST		REAL	TEST		REAL	TEST	
	Mass (mg)	Mass Est. (mg)	Rel. Perf.	Mass (mg)	Mass Est. (mg)	Rel. Perf.	Mass (mg)	Mass Est. (mg)	Rel. Perf.	Mass (mg)	Mass Est. (mg)	Rel. Perf.
FIBER	0	0	NA	0	0	NA	5	38	756%	16	25	151%
FILM	0	0	NA	0	0	NA	0	0	100%	0	0	100%
FOAM	0	474	NA	0	233	NA	0	110	NA	0	148	NA
FRAGMENT	221	1789	808%	192	1061	551%	1396	1696	121%	485	1022	211%
PELLET	1314	1240	94%	1465	1742	119%	96	462	484%	25	213	868%
TOTAL	1536	3502	228%	1657	3036	183%	1497	2306	154%	526	1408	268%

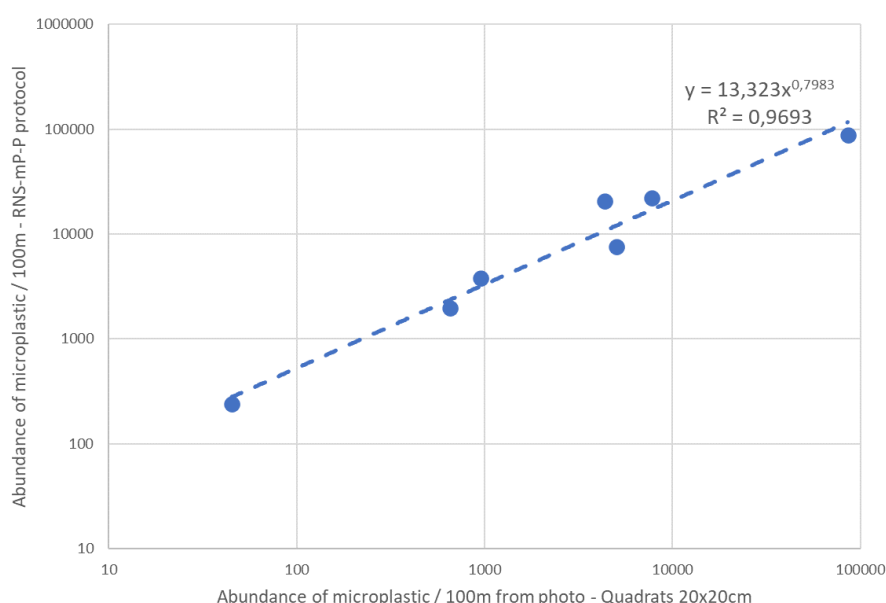
#### 4.4 Comparison with official monitoring results

Results obtained with AI-based analyses were compared with the official monitoring results obtained on the same site, during the same period, through the RNS-mP-P, in the context of the French national monitoring program for mesoplastics and large microplastics on beaches. Official results are expressed in numbers of microplastics or mesoplastics per 100 meters of beach.

Even though there are differences between the physical sampling protocol of the standardised RNS-mP-P method (which is also the EU-recommended methodology) and the photo-based sampling methods, the overall trends remain consistent, showing same phases of increasing and decreasing pollution along the coastline. In general, the quantification results obtained from photo analysis tend to be lower than those derived from the standardised RNS-mP-P protocol, which is explained by the different sampling strategies as RNS-mP-P/EU-recommended protocol consists in sampling over all the beach width, from the lowest wrackline to the back of the beach, providing a more integrative view of the pollution abundance on the beach. This indicates that the photo



acquisition strategy on the beach should be further optimised to make the two monitoring approaches more comparable and bring the figures closer between them.



**Figure 37: Relationship between the abundance of meso- and microplastics per 100 m of beach, as determined by the standardised RNS-mP-P method, versus the abundance derived from 20x20 cm quadrat photo analysis. Data from surveys between January 2023 and July 2024. The strong regression coefficient indicates a consistent correlation between the two methods**

Despite these differences, a strong regression relationship links the two approaches, with a very high correlation coefficient ( $R^2 = 0.9693$ ). Such a strong correlation suggests that AI-based photo analysis can serve as a complementary approach to support the monitoring of mesoplastics and large microplastics on beaches.

Finally, regarding the acquisition process and considering results presented in previous sections, to optimize time, it may be possible to reduce the number of photos.

## 5 Conclusion

In this study, the potential of AI-based imagery to optimise the monitoring of microplastics on a large number of samples in the context of a routine beach monitoring as recommended in MSFD TG-ML (2023), was assessed using a workflow developed by IFPEN.

The original recommended method consists in manual sampling followed by visual sorting and counting in the laboratory of each sample whereas the alternative methods tested consist in taking photographs of the main wracklines directly in the field and analysing the photos with AI-based imagery, in order to detect the number of particles





and their type in each photo and make an estimation of particles numbers in the wracklines.

Results were optimistic although some constraints were observed.

The relative proportions between different plastic categories are well maintained—if a particular type of microplastic is more prevalent in physical surveys, the AI analysis of photo data reflects the same trend. Additionally, the temporal variations identified by the AI align well with those observed in physical surveys, meaning the AI effectively tracks increases and decreases in meso- and microplastic pollution over time. A specific regression was identified between abundance derived from physical surveys and abundance derived from photo interpretation. Even though the values calculated by the AI, both in terms of mass and number, do not perfectly match those obtained through physical surveys on monitoring networks, they remain highly consistent.

The classification of films remains particularly challenging. Transparent films blend with the sandy background, making them difficult to differentiate, while opaque films share similar characteristics with fragments in 2D images. A potential improvement would be to merge the film category with fragments, acknowledging that part of this expanded fragment class includes films.

Results obtained revealed disappointing performance in transferring the AI's learning from one imagery survey (T2) to other surveys (T3, T4, T13, and T14). This highlights the need for a significantly larger and more diverse training dataset, incorporating a wider range of lighting conditions, backgrounds, and a balanced representation of different plastic forms.

Interestingly, simply adding more labelled data did not enhance AI performance. Between the first and second training phases, additional labelled images from surveys T3, T4, T13, and T14 were included to refine predictions. However, instead of improving accuracy, this expansion led to a decline in performance across training, validation, and test datasets, with a noticeable increase in false positives. This counterintuitive outcome suggests that further research is necessary. A promising approach would be to significantly expand the training set, not just in volume but also in diversity, ensuring a broader range of backgrounds and microplastic variations.

Optimizing the acquisition protocol by reducing the number of photos without compromising result quality is also a significant finding of the present work. This can lead to time and resource savings, making large-scale monitoring more feasible in time and space.

Therefore, obtained results show that the tested method has the potential to meet the requirements of both the EU-recommended and French monitoring program methodologies, in terms of particle counting and characterization and it should be further tested on other monitoring sites with different beach characteristics. However, the photo acquisition strategy on the beach currently differs from the EU-recommended



one and it should be further optimised to make the two monitoring approaches more comparable.

Based on its performance in the field, the tested methods also offer interesting perspectives to optimise analyses conducted in the lab, as a complement to the traditional imagery tools such as the ones tested in the Part 1 of the present study. For example, the tested approach could allow a direct analysis of raw sample (with organic matter) saving sample cleaning and sorting time.

In addition, capturing photos for monitoring a network offers a significant advantage because it constitutes a measurement rather than a sample. In the case of microplastics, physical sampling affects subsequent measurements, as the collected particles are permanently removed from the environment. This impact is rarely considered, and the influence of sampling on future measurements remains largely unassessed. Unlike traditional sampling, which alters the natural system, photographic monitoring allows for repeated measurements without interfering with the natural processes that transport, redistribute, and remove microplastics within the studied environment. This non-invasive approach thus enables more frequent and extensive data collection while preserving the integrity of the system.

Overall, while further improvements are needed—particularly in refining the AI's ability to classify rarer forms such as foams and fibers—this version of the AI methodology could already provide reliable indicators for long-term monitoring, in particular, in terms of particle detecting, counting and characterisation.





## References

Gauci, A; Deidun, A; Montebello, J; Abela, J; Galgani, F (2019) Automating the characterisation of beach microplastics through the application of image analyses. In: Ocean & Coastal Management, vol. 182, p. 104950. DOI: 10.1016/j.ocecoaman.2019.104950.

CEDRE (2024). French national monitoring network for mesoplastics and large microplastics on beaches. 2023 campaign report. Report R.24.26.C.

CEDRE (2025). Plastic pellets: loss prevention on industrial sites and response in the environment, 92p (Operational guide).

Cowger W, Gray A, Christiansen SH, DeFrond H, Deshpande AD, Hemabessiere L, Lee E, Mill L, Munno K, Ossmann BE, Pittroff M, Rochman C, Sarau G, Tarby S, Primpke S. Critical Review of Processing and Classification Techniques for Images and Spectra in Microplastic Research. Appl Spectrosc. 2020 Sep;74(9):989-1010. doi: 10.1177/0003702820929064. PMID: 32500727.

de Vries, R., Egger, M., Mani, T., Lebreton, L., 2021. Quantifying floating plastic debris at sea using vessel-based optical data and artificial intelligence. Remote Sensing 13 (17), 3401.

Lorenzo-Navarro, Javier; Castrillon-Santana, Modesto; Santesarti, Enrico; Marsico, Maria de; Martinez, Ico; Raymond, Eugenio et al. (2020) SMACC: A System for Microplastics Automatic Counting and Classification. In : IEEE Access, vol. 8, p. 25249–25261. DOI: 10.1109/ACCESS.2020.2970498.

Lorenzo-Navarro, Javier; Castrillón-Santana, Modesto; Gómez, May; Herrera, Alicia; Marín-Reyes, Pedro A. (2018) Automatic Counting and Classification of Microplastic Particles: Proceedings of the 7th International Conference on Pattern Recognition Applications and Methods. 7th International Conference on Pattern Recognition Applications and Methods. Funchal, Madeira, Portugal, 16/01/2018 - 18/01/2018: SCITEPRESS - Science and Technology Publications, p. 646–652.

Lorenzo-Navarro, J., Castrillón-Santana, M., Sánchez-Nielsen, E., Zarco, B., Herrera, A., Martínez, I., Gómez, M., 2021. Deep learning approach for automatic microplastics counting and classification. Sci. Total Environ. 765, 142728. <https://doi.org/10.1016/j.scitotenv.2020.142728>

Massarelli, Carmine; Campanale, Claudia; Uricchio, Vito Felice (2021) A Handy Open-Source Application Based on Computer Vision and Machine Learning Algorithms to Count and Classify Microplastics. In : Water, vol. 13, n° 15, p. 2104. DOI: 10.3390/w13152104.

Moorton et al. (2021) Is the use of Deep Learning and Artificial Intelligence an appropriate means to locate debris in the ocean without harming aquatic wildlife? Marine Pollution Bulletin, 181:113853, 2022.



MSFD TG-ML (2023), Galgani, F., Ruiz-Orejón, L. F., Ronchi, F., Tallec, K., Fischer, E. K., Matiddi, M., Anastasopoulou, A., Andresmaa, E., Angiolillo, M., Bakker Paiva, M., Booth, A. M., Buhhalko, N., Cadiou, B., Clarò, F., Consoli, P., Darmon, G., Deudero, S., Fleet, D., Fortibuoni, T., Fossi, M.C., Gago, J., Gérigny, O., Giorgetti, A., González-Fernández, D., Guse, N., Haseler, M., Ioakeimidis, C., Kammann, U., Kühn, S., Lacroix, C., Lips, I., Loza, A. L., Molina Jack, M. E., Norén, K., Papadoyannakis, M., Pragnel-Raasch, H., Rindorf, A., Ruiz, M., Setälä, O., Schulz, M., Schultze, M., Silvestri, C., Soederberg, L., Stoica, E., Storr-Paulsen, M., Strand, J., Valente, T., van Franeker, J., van Loon, W. M. G. M., Vighi, M., Vinci, M., Vlachogianni, T., Volckaert, A., Weiel, S., Wenneker, B., Werner, S., Zeri, C., Zorzo, P., and Hanke, G., Guidance on the Monitoring of Marine Litter in European Seas An update to improve the harmonised monitoring of marine litter under the Marine Strategy Framework Directive, EUR 31539 EN, Publications Office of the European Union, Luxembourg, ISBN 978-92-68-04093-5, doi:10.2760/59137, JRC133594.

OSPAR, van Franeker, J.A., (2015). Coordinated Environmental Monitoring Programme (CEMP) Guidelines for Monitoring and Assessment of plastic particles in stomachs of fulmars in the North Sea area. Agreement 2015-03.

Rodrigues, C., Rodríguez, Y., Frias, J., Carriço, R., Sobral, P., Antunes, J., Duncan, E.M., Pham, C.K., (2024). Microplastics in beach sediments of the Azores archipelago, NE Atlantic. *Marine Pollution Bulletin* 201, 116243.

Rohais, S., Moreaud, M., Guillaume, D., 2022. Procédé pour détecter et caractériser des particules de plastique par traitement d'images. Brevet Français 22/09.791

Rohais, S., Armitage, J. J., Romero-Sarmiento, M.-F., Pierson, J.-L., Teles, V., Bauer, D., Cassar, C., Sebag, D., Klopffer, M.-H., Pelerin, M. (2024). A source-to-sink perspective of an anthropogenic marker: A first assessment of microplastics concentration, pathways, and accumulation across the environment. *Earth-Science Reviews* 254, 104822.

Ronneberger O., Fischer P., Brox T., (2015) U-net: Convolutional networks for biomedical image segmentation, in: *Medical Image Computing and Computer-Assisted Intervention (MICCAI)*, Vol. 9351 of LNCS, Springer, 2015, pp. 234–241.

Scavino et al. (2009) Application of automated image analysis to the identification and extraction of recyclable plastic bottles DOI: 10.1631/jzus.A0820788

Schneider, C. A., Rasband, W. S., & Eliceiri, K. W. (2012). NIH Image to ImageJ: 25 years of image analysis. *Nature Methods*, 9(7), 671–675. doi:10.1038/nmeth.2089

Simonyan K., Zisserman, A. (2014) Very deep convolutional networks for large-scale image recognition,” *CoRR*, vol. abs/1409.1556, 2014. [Online]. Available: <http://arxiv.org/abs/1409.1556>

Tan, Z., Moreaud, M., Alata, O., Atoo, A.M. (2018). ARFBF Morphological Analysis – Application to the Discrimination of Catalyst Active Phases. *Image Analysis and Stereology* 37(1), p. 21-34.

Turner, A., Wallerstein, C. Arnold, R. (2019). Identification, origin and characteristics of bio-bead microplastics from beaches in western Europe. *Science of The Total Environment* 664, 938-947.





van Lieshout, C., van Oeveren, K., van Emmerik, T., & Postma, E. (2020). Automated river plastic monitoring using deep learning and cameras. *Earth and Space Science*, 7, e2019EA000960. <https://doi.org/10.1029/2019EA000960>

Wahab, D. A., Hussain, A., Scavino, E., Mustafa, M. M. & Basri, H. (2006) Development of a Prototype Automated Sorting System for Plastic Recycling. *American Journal of Applied Sciences*. 3 (7), 1924-1928. Available from: <http://www.thescipub.com>. Available from: doi: 10.3844/ajassp.2006.1924.1928.

Wolf et al. (2020) Machine learning for aquatic plastic litter detection, classification and quantification (APLASTIC-Q) <https://doi.org/10.1088/1748-9326/abbd01>

Wu et al. (2020) Auto-sorting commonly recovered plastics from waste household appliances and electronics using near-infrared spectroscopy <https://doi.org/10.1016/j.jclepro.2019.118732>

Zhu et al. (2021) Microplastic pollution monitoring with holographic classification and deep learning <https://doi.org/10.1088/2515-7647/abf250>

